Sveriges lantbruksuniversitet
Swedish University of Agricultural Sciences

Faculty of Veterinary Medicine and Animal Science
Department of Animal Breeding and Genetics

Generating Large-Scale Conditional Knock-In Mouse Models using CRISPR/Cas9 in Embryonic Stem Cells

Gus Rowan McFarlane

Examensarbete / Swedish University of Agricultural Sciences
Department of Animal Breeding and Genetics

511

Uppsala 2016

Master's Thesis, 30 ECTS

Erasmus Mundus

Sveriges lantbruksuniversitet
Swedish University of Agricultural Sciences

Faculty of Veterinary Medicine and Animal Science
Department of Animal Breeding and Genetics

Generating Large-Scale Conditional Knock-In Mouse Models using CRISPR/Cas9 in Embryonic Stem Cells

Gus Rowan McFarlane

Supervisors:
Göran Andersson, SLU, Department of Animal Breeding and Genetics
Ben Davis, University of Oxford, Nuffield Department of Medicine

Examiner:
Magnus Åbrink, SLU, Department of Biomedical Science and Veterinary Public Health

Credits: 30 ECTS
Course title: Degree project in Animal Science
Course code: EX0556
Programme: Erasmus Mundus
Level: Advanced, A2E

Place of publication: Uppsala
Year of publication: 2016
Title of series: Examensarbete / Swedish University of Agricultural Sciences, Department of Animal Breeding and Genetics, 511
Online publication: http://stud.epsilon.slu.se

Keywords: CRISPR/Cas9, Conditional Knock-In mice, Transgenic mice, Fbxw7, Colorectal cancer

Generating Large-Scale Conditional Knock-In Mouse Models using CRISPR/Cas9 in Embryonic Stem Cells

by

GUS ROWAN MCFARLANE

BSc, Royal Melbourne Institute of Technology University, 2014

A THESIS

submitted in partial fulfillment of the requirements for the degree

MASTER OF SCIENCE IN ANIMAL SCIENCE

Department of Animal Breeding and Genetics
Faculty of Veterinary Medicine and Animal Science

SWEDISH UNIVERSITY OF AGRICULTURAL SCIENCES
Uppsala, Sweden

2016

supervised by

PROFESSOR GÖRAN ANDERSSON
DR BEN DAVIES

Abstract

The discovery and repurposing of CRISPR/Cas9 has revolutionized the field of genome editing and allowed for the development of mouse models with unprecedented simplicity and speed. The application of CRISPR/Cas9 in mouse embryonic stem cells represents a highly efficient and well-established method for generating large-scale conditional knock-in mouse models. This study employed a CRISPR/Cas9-mediated gene targeting approach in mouse embryonic stem cells to introduce a conditional knock-in construct within intron 11 of the Fbxw7 gene. Fbxw7 is mutated in a diverse range of human cancers, including colorectal cancer. As existing mutant Fbxw7 mouse models carry null alleles, the aim of this study was to create a mouse model carrying one of the commonly occurring point mutations in human cancers (Fbxw7(R482Q)). The construct integrated into the genome of mouse embryonic stem cells was a 5.5 kb Cre-dependent conditional knock-in that harboured the Fbxw7(R482Q) mutant allele and a cyan fluorescent protein reporter gene. Following screening and functional testing of the targeted embryonic stem cells, two confirmed clones were microinjected into wild type blastocysts. Subsequently, eight chimeric male mice were born from four litters. Two 95% male chimeras are currently breeding with wild type females in the hope of achieving germline transmission of the embryonic stem cell derived genes. Successful germline transmission will generate heterozygous *Fbxw7*^{R482Q} mice. Once a breeding population is established the *Fbxw7*^{R482Q} mice will be crossed with *Villin-Cre* mice to study the role Fbxw7(R482Q) in the development of colorectal cancer.

Table of Contents

List of Figures

List of Tables

List of Abbreviations

cCRISPR	gRNA subcloned CRISPR expression plasmid
CRISPR	Clustered Regularly Interspersed Palindromic Repeats
crRNA	CRISPR RNA
dH_2O	Distilled water
dNTPs	Deoxynucleotide triphosphates
DSB	Double-stranded DNA Breaks
EDTA	Ethylenediaminetetraacetic acid
EMFOL	Erasmus Mundus Food of Life Masters Programme
FCS	Foetal calf serum
Floxed	An allele that is flanked by *loxP* sites
GE	Gel electrophoresis
GFP	Green fluorescent protein
GM	Genetically modified
gRNA	Single guide RNA
HDR	Homology directed repair
Indel	Insertion-deletion mutation
KI	Gene knock-in mouse model
KO	Gene knock-out mouse model
mESC	Mouse Embryonic stem cells
NHEJ	Non-homologous end-joining
PAM	Protospacer adjacent motif
PBS	Phosphate-buffered saline
PCR	Polymerase chain reaction
ssODN	Single stranded oligodeoxynucleotide
TALEN	Transcription activator-like effector nuclease
TAT-Cre	Cell permeable Cre recombinase
tracrRNA	Trans-activating CRISPR RNA
WP	Cell culture multiple well plate
WT	Wild type
WTCHG	Wellcome Trust Centre for Human Genetics at the University of Oxford
ZFN	Zinc finger nucleases

Acknowledgements

I would like to offer my sincere thanks and appreciation to my supervisor, Professor Göran Andersson from the Swedish University of Agricultural Sciences. Through his patience, support and exhaustive administrative efforts he has made this project possible.

I would also like to expression my deepest thanks to my co-supervisor, Dr Ben Davies from the Wellcome Trust Centre for Human Genetics (WTCHG) at the University of Oxford. Ben bravely offered me an internship in his group with the full understanding that I was 'numpty' to the world of mouse genetics and genome editing. Through his guidance and willingness to share his expertise, he has played a central role in developing this project and broadening my knowledge.

I am also very grateful for the unending advice and guidance provided by Alberto, Dan, Chris and Polinka during my time in laboratory at the WTCHG. My wet lab skills have significantly improved thanks to their valuable tuition.

This project has been undertaken as part of the Erasmus Mundus Food of Life Programme (EMFOL) and as such I would like to thank Professor Chris Knight and the EMFOL administrative team for their continual support throughout the programme. EMFOL has been an incredible experience for me.

Finally, to my family, it's impossible to adequately thank you for everything you've done.

1 Introduction

1.1 Genetically modified mice as human disease models

Genetically modified (GM) mice are used extensively in biomedical research for modelling human disease and studying gene function (Ittner & Delerue, 2015). As a model species, mice act as good analogues for most human biological processes since both species share up to 99% of the same genes. Mice also have the practical benefits of a short reproductive cycle, large litters, small physical size and relatively low maintenance costs. These benefits, in conjunction with the increasingly dense map of the mouse genome, the multitude of uniform inbred strains available and the establishment of mouse embryonic stem cells (mESCs) makes the laboratory mouse a powerful and indispensable model to study the genetic basis of diseases *in vivo* (Capecchi, 1994; Hall et al., 2009; Vandamme, 2015). In addition to studying the mechanistic consequences of disease-related genetic alterations, verified mouse models provide an important platform to develop new diagnostic and therapeutic strategies to combat these diseases (Peters et al., 2007).

The first GM mice were produced in the early 1980's by microinjection of plasmids encoding viral antigens into the genome of zygotes (Gordon et al., 1980; Palmiter et al., 1982). However, this rudimentary method was of no practical use for the detailed study of gene function or for developing disease models as integration occurred in a non-targeted manner and without copy number control. Pioneering work on DNA repair by homologous recombination (HR) during the mid 1980s (Folger et al., 1984) hinted at the prospect that it may be possible to target exogenous DNA to specific genomic loci by including a homologous sequence in targeting vectors. These findings, along with the isolation of mouse embryonic stem cells (mESCs; Martin, 1981) and advancements in the micromanipulation of embryos paved the way for a new strategy to introduce site specific modifications into the mouse genome: gene targeting.

1.2 Classical gene targeting

Gene targeting is defined as the introduction of site-specific modifications into the genome. Initial successes in the mid 1980's with gene targeting were accomplished by microinjecting DNA

sequences with high homology to the targeted genomic sequence into cultured mammalian cells (Smithies et al., 1985). These experiments utilized a HR-dependent approach, which took advantage of the cell's own DNA repair machinery to replace a targeted genetic locus with an introduced DNA sequence. However, the targeting events occurred at very low rates (1 in $3x10^4$ cells) making it unfeasible to efficiently target zygotes to generate GM mice using this approach (Capecchi, 1989). At the time, mESC had been recently isolated (Martin, 1981) and researches capitalised on this breakthrough. By using HR-dependent gene targeting in mESCs, scientists could transfect, select and screen for clones carrying the alteration of interest. The most common selection method was to include a positive selection cassette, such as the neomycin resistance gene in targeting vector. After selection in antibiotics and screening, positive mESC clones could be expanded and microinjected into WT blastocysts, in the hope that they contribute to the germ cells of the resulting chimeric offspring (Behringer et al., 2014; Hughes & Saunders, 2011; Müller, 1999). Germline competent chimeras could then be bred to produce mice carrying the alteration of interest.

As classical gene targeting in mESCs developed, scientist defined three broad classes of GM mice. These are still in use today and are: 'knock-out', 'knock-in' and 'conditional' gene targeted mice. In knock-out (KO) mice, a gene is inactivated so that it is no longer functional, whereas in knock-in (KI) mice, exogenous DNA is added to the genome to modify genetic behaviour. With conditional gene targeting a genetic 'switch' is introduced that limits KO or KI mutations to be active only in specific cells, or at a specific developmental stage (Doyle et al., 2012; Seruggia & Montoliu, 2014). These classes of mouse models have contributed greatly to our understanding of gene function and genetic basis of disease. However, these classes where established upon classical gene targeting protocols in mESCs, which did not allow for the high throughput mouse model production that researchers demanded. The technology's inefficiencies were due to the low frequencies with which homologous templates were incorporated into the genome and complicated by off-target vector integration, requiring time and labour-intensive screening procedures by Southern blotting to ensure correct clone selection. Furthermore, the construction of mouse models carrying multiple alterations added substantially more time, cost and effort (Rocha-Martins et al., 2015).

1.3 Double stranded DNA breaks stimulate gene targeting

A key breakthrough for increasing production efficiency was the realization that double-stranded DNA breaks (DSBs) greatly stimulated cellular DNA repair mechanisms (Rouet et al., 1994; Smih et al., 1995). All eukaryotic cells efficiently repair DSBs using one of two pathways: non-homologous end-joining (NHEJ) or a via a form of HR, known as homology directed repair (HDR). The former simply joins the broken ends of the DNA, often creating small insertion or deletion mutations (indels); the latter uses a homologous DNA template to replace the broken region with high fidelity. Thus, the induction of directed DSBs at a genomic locus of interest can greatly stimulate gene targeting efficiency. As targeted DSBs in the genome could be introduced by nucleases, this method has become known as nuclease-assisted gene targeting (Singh et al., 2015; Yang, Wang, & Jaenisch, 2014). For KO mice, using the error-prone NHEJ pathway frequently results in indel mutations. Indels located within protein-coding exons can cause frameshifts resulting in a KO allele. Whilst to achieve KI alleles, donor DNA plasmid or single-strand oligodeoxynucleotide (ssODN) repair template with homology arms up and downstream of the DSB can be used to insert an exogenous DNA sequence via HDR (Chandrasegaran & Carroll, 2016; Kim & Kim, 2014; Figure 1.1).

Early nuclease-assisted gene targeting experiments using rare-cutting meganucleases demonstrated that DSBs increased the frequency of template integration in mESCs by at least 2 to 3 orders of magnitude (Rouet et al., 1994). Although this substantial increase in efficiency was a significant advance, the practical utility of meganucleases to target any genomic loci at will was limited by the long and highly specific DNA recognition sequences (14 to 40 bp) of these enzymes. Furthermore, the engineering of meganucleases was extremely challenging for the majority of researchers because the DNA recognition sites and cleavage functions of these enzymes are intertwined in a single domain (Rocha-Martins et al., 2015; Sander & Joung, 2014). However, the possibility of manipulating genomes at will captivated scientist's attention and the initial challenges posed by meganucleases were soon overcome by the development of a new genre of truly programmable nucleases; which made it possible to generate DSBs at almost any given genomic loci.

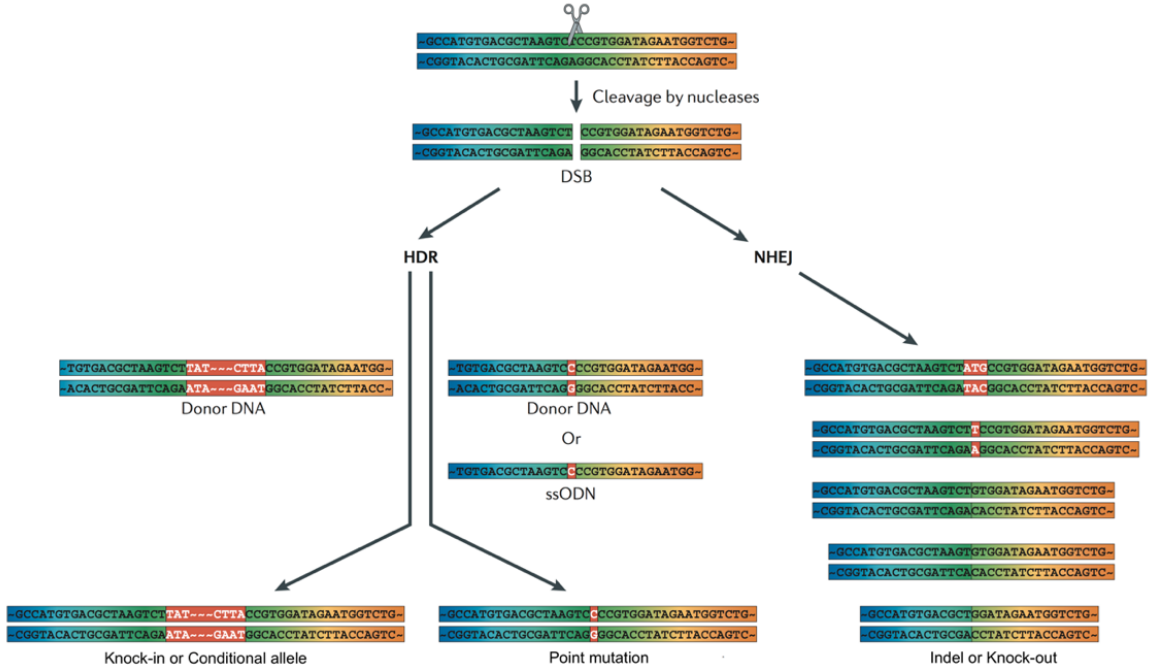

Figure 1.1 Nuclease-assisted gene targeting. Double strand DNA breaks (DSBs) from site specific nucleases could lead to sequence insertion (red box) through homology directed repair (HDR) in the presence of a donor DNA plasmid or a single-strand oligodeoxynucleotide (ssODN), both of which must contain homology arms. DSBs can also be repaired through non-homologous end joining (NHEJ), which frequently leads to small insertions and deletions (indels). Image modified and adapted from Kim and Kim (2014).

1.4 Programmable nucleases systems

Programmable nucleases have transformed the field of genome editing. This class of nucleases can be engineered to bind to a specific nucleotide sequence in the genome and subsequently generate a DSBs for gene targeting at a user defined site. Currently, there are three programmable nuclease systems used for gene targeting in mice - zinc finger nucleases (ZFNs), transcription activator-like effector nucleases (TALENs) and clustered regularly interspaced short palindromic repeats/CRISPR-associated protein (CRISPR/Cas) - with the latter quickly gaining prominence due to its ease of use. Each of these programmable nuclease systems fundamentally consists of two key elements: a DNA recognition domain conferring target specificity and a nuclease domain for DNA cleavage (Kim & Kim, 2014; Rocha-Martins et al., 2015). A description of ZFNs, TALENs and the now ubiquitously used CRISPR/Cas9 system is provided below.

1.4.1 ZFNs (1996)

A ZFN is comprised of a DNA-binding zinc finger protein (ZFP) domain and a non-specific nuclease domain derived from the FokI restriction enzyme. Each zinc-finger recognizes a 3 bp DNA sequence in the genome, and 3 to 6 zinc fingers are typically used to generate a single ZFN subunit that binds to DNA sequences of 9 to18 bp (Figure 1.2). Importantly, the DNA-binding specificities of zinc fingers can be engineered, which is an essential feature for programmable nucleases. To achieve DNA cleavage, the modified FokI domain used in ZFNs must be dimerize. Thus, two ZFN monomers are required to form an active nuclease and each monomer must bind to adjacent half-sites that are separated by spacers of 5 to 7 bp. After binding of the ZFNs the pair of FokI nucleases dimerize and generate a DSB with 5′ overhangs. While ZFNs can in theory target any genomic sequence, the difficulty of accurately predicting protein conformation and DNA-protein interactions make ZFN construction a tedious and costly process, involving a substantial validation phase prior to application. As such, ZFNs have been restricted to developing GM mouse models in only a minority of highly specialized labs (Kim & Kim, 2014; Urnov et al., 2010).

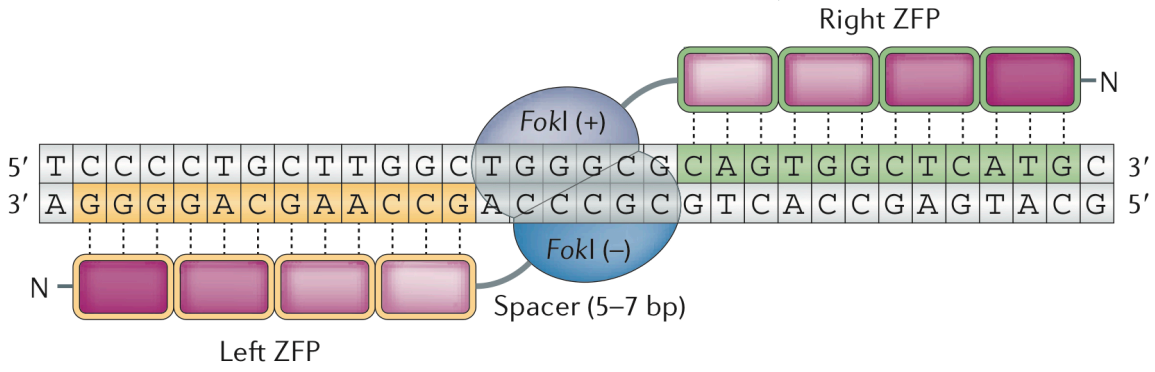

Figure 1.2 A schematic representation of zinc finger nuclease (ZFN) structure. Each ZFN is composed of a zinc-finger protein (ZFP) DNA binding domain and a FokI nuclease domain. Image modified and adapted from Kim and Kim (2014).

1.4.2 TALENs (2010)

An analogous but simpler alternative to ZFNs was developed following the deciphering of the DNA recognition patterns of transcription activator-like effector proteins (TALEs). The general structure of TALENs is similar to that of ZFNs (Figure 1.3). Like ZFNs, TALENs contain the FokI

nuclease domain but use a different class of DNA binding domains known as TALEs, which are derived from *Xanthomonas* spp. bacterium. TALEs are composed of tandem arrays of 33 to 35 amino acid repeats, each of which recognizes a single base-pair. The nucleotide specificity of each repeat domain is determined by the two amino acids at positions 12 and 13, which are called repeat variable diresidues (RVDs). Although the single base discrimination of TALE modules compared to 3 bp recognition in zinc fingers provides less limitations on target selection, the inherently repetitive nature of TALE repeats poses a challenge when assembling the DNA molecules to encode these proteins. As with ZFNs, TALENs are intrinsically dependent on protein-DNA interactions to drive specificity. Due to this dependency, TALENs also require extensive *in vitro* validation as protein conformation often varies depending on the specific context of use. Nonetheless, the greater simplicity of TALENs compared to ZFNs has led a broad range of laboratories utilizing this technology to generate GM mouse models (Gaj et al., 2013; Gupta & Musunuru, 2014; Kim & Kim, 2014).

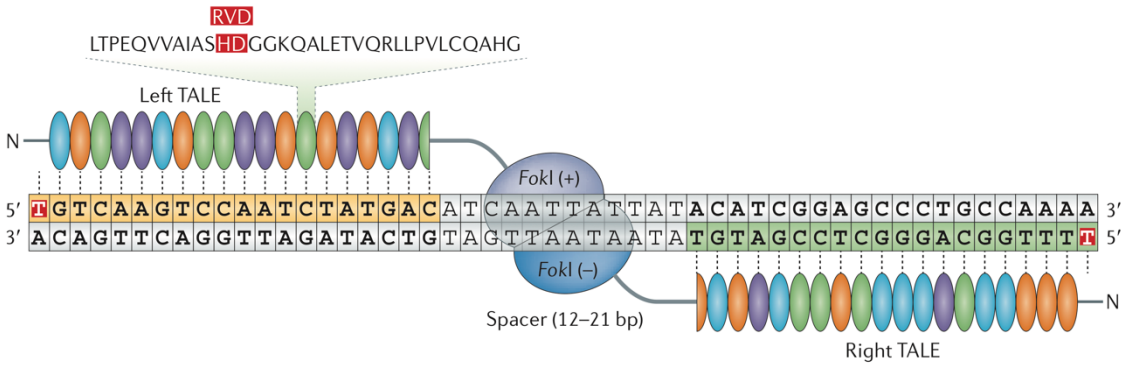

Figure 1.3 A schematic representation of transcription activator-like effector nuclease (TALEN) structure. Each TALEN is composed of DNA binding TALE domain and a FokI nuclease domain. Each TALE repeat is comprised of 33–35 amino acids and recognizes a single base pair through the amino acids at positions 12 and 13, which is called the repeat variable diresidue (RVD; shown in red). Image sourced from Kim and Kim (2014).

1.4.3 CRISPR/Cas9 (2012)

The discovery of bacterial adaptive immune systems known as CRISPR/Cas systems has led to the latest set of genome editing tools. These tools have overcome many of the technical challenges researchers faced when using ZFNs and TALENs. The RNA-guided CRISPR/Cas system was first observed in *E. coli* in 1987 by its striking genomic structure (Ishino et al., 1987). Evolved as an

adaptive immune system in bacteria and archaea, the system uses a set of *Cas* genes to incorporate exogenous DNA into the CRISPR locus, and subsequently transcribe them as RNA templates that guide the Cas proteins to cleave invasive DNA or RNA (Horvath & Barrangou, 2010). However, the system was not repurposed into a genome editing tool until 2012 when Jinek et al. published their seminal paper. Three types of CRISPR/Cas systems have been identified to date, differing in their targets as well as mechanisms of action. Type I and III CRISPR systems employ an ensemble of *Cas* genes to carry out RNA processing, targeting, and target site cleavage. By contrast, the type II CRISPR/Cas system makes use of a single nuclease, Cas9, to cleave target DNA. Among the three types of CRISPR/Cas systems, the type II CRISPR/Cas9, derived from *Streptococcus pyogenes* is presently the most suitable and widely used as a genome editing tool (Chandrasegaran & Carroll, 2016; Mojica & Montoliu, 2016; Moore, 2015).

The *S. pyogenes* type II CRISPR/Cas9 system consists of a SpCas9 nuclease and two RNAs; CRISPR RNA (crRNA) and trans-activating CRISPR RNA (tracrRNA). SpCas9 is directed to the target site by the 20 nt crRNA and the required auxiliary tracrRNA. The crRNA sequence directs SpCas9 to the target site by Watson-Crick base-pairing with the target DNA sequence (Cong et al., 2013). However, for most genome editing applications the crRNA and tracrRNA are fused to form a 102 nt single guide RNA (gRNA). In addition to the crRNA providing specificity, a protospacer adjacent motif (PAM), a defined 3 nt sequence at the 3' end of the target DNA sequence must be present for DNA cleavage to occur . For SpCas9, the PAM sequence is 5'-NGG, which on average occurs every 10 bp in the mouse genome. At an overall structural level, SpCas9 contains two nuclease domains, HNH and RuvC, each of which cleaves one strand of the target DNA (Figure 1.4). In SpCas9, these domains cleave 3 bp upstream from the PAM sequence, leaving blunt ends (Hsu et al., 2013; Singh et al., 2015). As the PAM requirements of SpCas9 limits the potential target sites, CRISPR/Cas9 systems from other species with different PAM sequences have been employed for gene targeting mammalian cells (44, 53, 54). For example, the *Neisseria meningitidis* Cas9 PAM has been reported to be 5'-NNNNGATT (Hou et al., 2013).

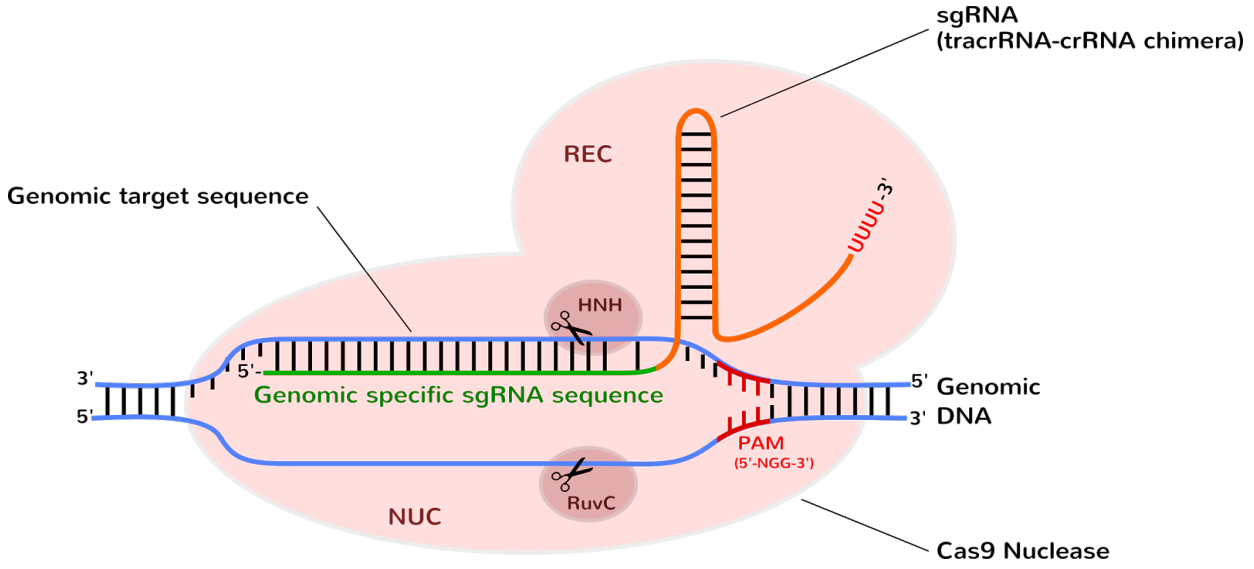

Figure 1.4 A schematic representation of *Streptococcus pyogenes* CRISPR-associated protein-9 (SpCas9) structure, which is programmed with a single guide RNA (gRNA). gRNA comprises a site specific CRISPR RNA (crRNA; green) and an auxiliary trans-activating crRNA (tracrRNA; orange). After the gRNA and SpCas9 bind to the target site, the recognition (REC) and nuclease lobes (NUC) undergo rotation to fully enclose the DNA target sequence. Two nuclease domains (RuvC and HNH) each cut one DNA strand 3 bp upstream from the protospacer adjacent motif (PAM) to generate a double strand DNA break (DSB). Image sourced from ozbiosciences.com.

In contrast to ZFNs and TALENs, which require the design of proteins that are encoded by large repetitive DNA segments (500 to 1500 bp) for each new target site, CRISPR/Cas9 can be easily adapted to target almost any genomic sequence by simple exchanging the 20 nt crRNA. This can be easily accomplished by subcloning the 20 nt sequence into a gRNA expression plasmid. The SpCas9 protein component remains unchanged, alleviating the need for complex protein engineering. Like previous programmable nucleases, CRISPR/Cas9 provides highly efficient and precise genome editing capabilities in mice (Gupta & Musunuru, 2014). CRISPR/Cas9 induced mutation rates of up to 78% have been obtained in mice (Fujii et al., 2013; Yang, Wang, Shivalila, et al., 2014). However, the most significant advantage that CRISPR/Cas9 offers over ZFNs and TALENs is that it uses reagents that are simple, cheap, and quick to design and generate (Gupta & Musunuru, 2014). Furthermore, since the repurposing of CRISPR/Cas9 as a genome editing tool several technological innovations have evolved from the technology. These include: multiplexing mutations with several gRNAs in a single step (Cong et al., 2013), the development of a paired Cas9 'nickase' system (Shen et al., 2014), dimerizing of dCas9 (dead Cas9; catalytically inactive) system fused with a FokI endonuclease (Tsai et al., 2014), and adding a DNA-binding domain for

improved target specificity (Bolukbasi et al., 2015). With these successive innovations, the CRISPR/Cas9 system has become widely adapted for a multitude of genome editing applications.

1.5 Gene targeting with CRISPR/Cas9

The efficiency of CRISPR/Cas9 as a genome editing tool has allowed for gene targeting by direct microinjection into zygotes. For the development of KO and simple KI mouse models this alleviates the cost and labour required with mESC technology (Singh et al., 2015). Although ZFNs and TALENs also have this ability. The standard method for generating KO alleles using CRISPR/Cas9 is co-injection of Cas9 mRNA and gRNA into the pronucleus and/or cytoplasm of mouse zygotes. Alternatively, pronuclear injection of recombinant Cas9 protein in complex with gRNA (Ribonucleoprotein (RNP)) has also proven to be very effective for generating KO alleles (Chen et al., 2016; Williams et al., 2016; Table 1.1) In both cases, the gRNA is directed to a protein coding exon in the target gene. Once a DSB is induced at the target site it is favourably repaired by NHEJ, which is the most active repair pathway in mammalian cells. The error prone NHEJ pathway frequently results to small indels that ideally cause a frameshift in the protein-coding exon and consequently a loss-of-function mutation within the targeted gene (Gaj et al., 2013). Targeted zygotes are then transferred into foster mothers to develop in KO mouse models.

The production of simple KI mouse models by direct microinjection is similar to KO model production but requires the inclusion of a repair template. In addition to Cas9 (mRNA or RNP) and gRNA, a ssODN template is also required to induce the cell to repair the DSB by HDR. One important consideration in ssODN design is ensure the gRNA target site or PAM is altered after integration of the targeting vector by HDR. This will prevent recurrent cleavage of the target site, which could lead to undesirable mutations (Singh et al., 2015; Williams et al., 2016). Scientists have been consistently successful in generating CRISPR/Cas9-mediated KI alleles in zygotes with ssODN template lengths ranging from 100 to 200bp in total, with at least 40 bp homology arms on either side of your intended DSB (Rappaport & Johnson, 2014; Skarnes, 2015). Recently, Yoshimi et al. (2016) successfully achieved a 1kb KI using a long synthetic ssODN but this technique requires further investigation before widespread application is seen.

Researchers have embraced direct CRISPR/Cas9 microinjection of zygotes for generating KO and rudimentary KI mouse models. Although direct zygote injection is effective for simple KI alleles, the generation of larger more complexed KI alleles requires HDR with a donor DNA plasmid, which is difficult to produce by direct zygote injection (Skarnes, 2015). In a study by Yang, Wang, and Jaenisch (2014), they reported that only 10 to 30% of zygotes co-injected with CRISPR/Cas9 and donor plasmids carried the desired modification. As such, the 'gold standard' for generating large-scale KI mouse models remains the well-established mESC technology (Chen et al., 2016). With this approach a CRISPR expression plasmid (Table 1.1) and donor DNA plasmid is electroporated into mESCs. Donor plasmids typically consist of homology arms (each >800 bp), the KI cassette of interest and selection markers, such as antibiotics resistance or fluorescent proteins for identifying successfully transfected cells. Following selection, researchers can screen and expand positive clones for injection into WT blastocysts to generate chimeric offspring for germline transmission (Singh et al., 2015; Wang et al., 2015). Although more laborious and costly than direct gene targeting in mouse zygotes, the proven ability of mESC technology to handle complex KI alleles is yet to be rivalled by direct zygote microinjection (Skarnes, 2015).

Table 1.1 Components and applications of CRISPR/Cas9 expression systems used for generating genetically modified mouse models.

Expression system	Components of system	Application
CRISPR expression plasmid	Promoter driving Cas9 expression can be constitutive or inducible. U6 promoter is typically used for expressing gRNA in the same plasmid. May contain a selection marker (e.g. neomycin resistance) to generate stable cell lines.	Transient expression of Cas9 and gRNA in mammalian cells which can be transfected via electroporation at high efficiency. Commonly used for gene targeting in mESCs.
Cas9 mRNA and gRNA	Plasmids containing gRNA and Cas9 are used in *in vitro* transcription reactions to generate Cas9 mRNA and gRNA, then delivered to target cells.	Transient expression of CRISPR/Cas9 components, expression decreases as RNA is degraded within the cell. Typically microinjected directly into zygotes.
Ribonucleoprotein(RNP)	Purified Cas9 protein and in vitro transcribed gRNA are combined to form a Cas9/gRNA complex and delivered to cells.	Transfection of cells via microinjection or electroporation. Instant CRISPR/Cas9 activity, with expression decreasing as RNP is degraded within the cell.

Note:1) CRISPR/Cas9 can also be expressed via viral transduction systems, however, these systems are not currently used for generating GM mice.
2) Information within this table was sourced from: Behringer et al. (2014), Chen et al. (2016) and Sato et al. (2016)

1.6 Conditional gene targeting

Conventional KO and KI gene targeting strategies are effective for developing a wide variety of GM mouse models. However, the role of many mutations cannot be investigated due to early lethal phenotype preventing the study of its later roles or the phenotype affects multiple tissues, preventing the detailed study of its function in a particular tissue or organ. To overcome this issue, the application of site specific recombinase systems has made it possible to 'switch on' mutations in specific cells or at a specific developmental stage (Bayascas et al., 2006; Kwan, 2002; Tahimic et al., 2013). Site-specific recombinase systems consist of two basic elements: the recombinase enzyme and a DNA sequence that is specifically recognized by that particular recombinase. Recognition is through a consensus sequence and the recombinase catalyses recombination between two of its recognition sites to bring about genome modification. Currently, there are two recombinase systems used in mouse gene targeting experiments: Cre-*loxP* and Flp-*FRT* systems (Kwan, 2002).

The Cre/*loxP* system, derived from the P1 bacteriophage and the Flp-*FRT* system from *Saccharomyces cerevisiae* are used for generating conditional alleles in mouse models. Each of these recombinases (Cre or Flp) recognizes a 34-bp consensus sequence consisting of two 13 bp palindromic sequences (Cre or Flp recognition sites) and an 8 bp non-palindromic core that is responsible for the directional nature of the recognition site (*loxP* or *FRT*; Figure 1.5a; Kwan, 2002). Flp/*FRT* is less frequently employed due to its lower efficiency (Meyers et al., 1998). Therefore, for ease and clarity of explanation, herein, the focus will be on widely employed Cre/*loxP* system; although Flp/*FRT* can be used in many of the same strategies. Within Figure 1.5b, it can be seen that two *loxP* sites in the same direction will result in excision of the intervening DNA by Cre induced recombination, leaving one intact *loxP* site. In contrast, where two *loxP* sites are in the opposing directions, the recombinase will invert the intervening piece of DNA. The 34 bp *loxP* recognition site is very unlikely to occur at random in the mouse genome, yet is small enough to be considered a 'neutral' sequence when integrated into the mouse genome (Kwan, 2002).

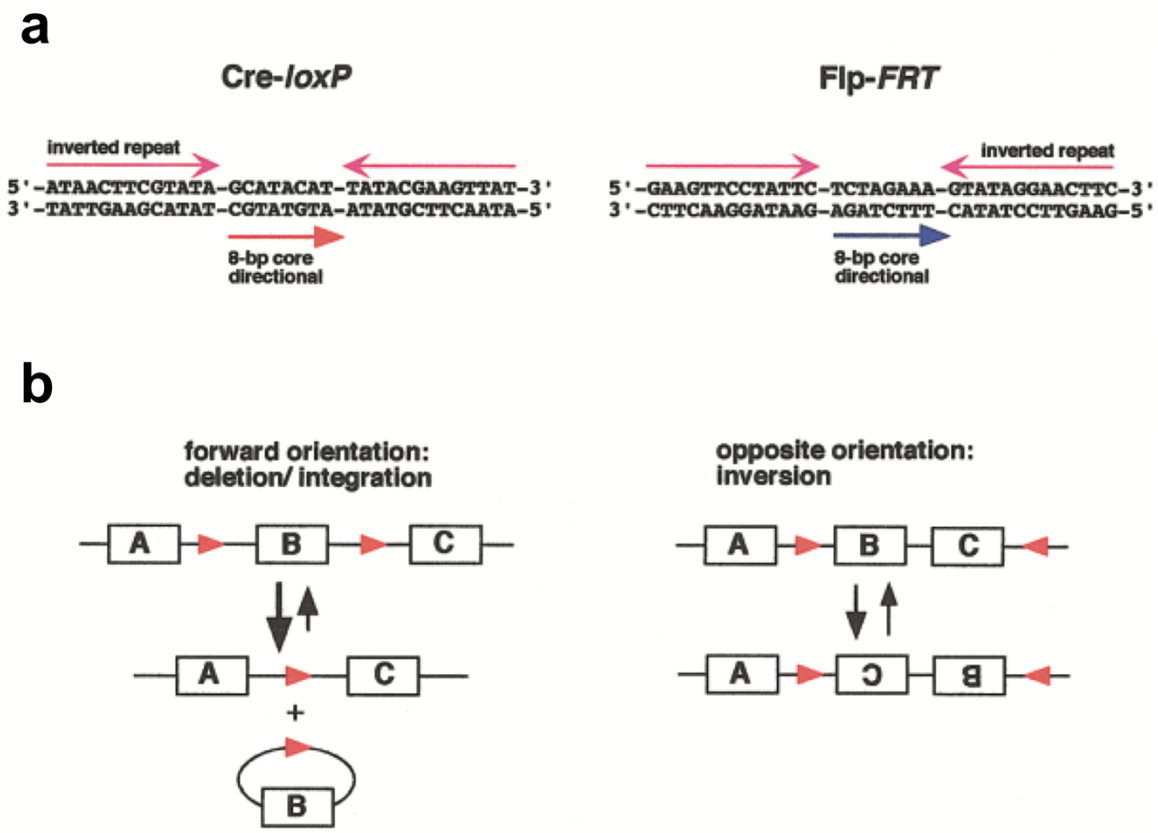

Figure 1.5 Site-specific recombinase systems (a) Structure and sequence of the *loxP* and *FRT* recombinase recognition sites. Each site consists of two 13 bp inverted repeats flanking an asymmetric 8 bp core region that defines the directionality of the recognition site. (b) Digram of a deletion and inversion by Cre/*loxP* and Flp/*FRT* mediated recombination. Image was modified and adapted from Kwan (2002).

As targeting vectors for inserting Cre/*loxP* conditional alleles are very large, frequently exceeding 5 kb to include the intervening DNA sequence, they typically require the use mESCs and donor plasmids for efficient construct integration (Tahimic et al., 2013). To overcome the costly and laborious requirements of using mESCs for generating conditional mutant mice, Yang, Wang, Shivalila, et al. (2014) developed a 'one-step' CRISPR/Cas9-mediated method for generating flanked by *loxP* (floxed) alleles directly in mouse zygotes. Their method involves the simultaneous injection of Cas9 mRNA, two gRNAs targeted at desired *loxP* locations, and two corresponding ssODN templates encoding *loxP* sites and 60 nt homology arms surrounding the DSB sites. Using this strategy, the genome is cut twice at different genomic loci and separate *loxP* sites are integrated into the DSBs via HDR with ssODNs. Although this system reduces the cost, time and number of

mice required for generating conditionally mutant mice, to date the author is not aware of any other publications or reports of studies that have utilized this 'one-step' CRISPR/Cas9-mediated approach for generating conditional alleles directly in mouse zygotes. At present, it seems researchers are continuing to employ the well-established protocols of mESC technology to generate Cre/*loxP* conditional alleles.

There are three common strategies employed for generating conditional KI mouse models. These are: the 'heterozygous', 'minigene' and 'inversion' methods (Figure 1.6). In the heterozygous method, a mouse is generated that has one allele which comprises a floxed WT exon, whereas the second allele contains the KI mutant exon and is not floxed. In tissues that express Cre, the WT exon will be excised leaving only expression of the KI mutant allele (Figure 1.6a). The disadvantage of this method is that in non-Cre-expressing tissue both the mutant and WT protein is expressed. To avoid expression of mutant protein in non-Cre-expressing tissues, the minigene method can be employed. In this method, an allele is constructed in such a way that in the absence of Cre, an artificial version of the wild gene is expressed. This wild gene consists of an intronless minigene and STOP casette that are floxed. The construct is designed so that Cre-mediated recombination leads to the excision of the floxed minigene and STOP cassette, resulting in the expression of the KI mutant allele (Figure 1.6b). A third approach, called the inversion method, relies upon opposing orientations of *loxP* sequences. In the inversion method, the KI exon is cloned in an antiparallel orientation after the WT exon, and the WT and inverted KI exons are floxed (Figure 1.6c). In the absence of Cre, the WT exon will be expressed and the sequence within the inverted KI exon should be spliced-out of the pre-mRNA. In the presence of Cre recombinase, DNA inversion would result in the KI exon being expressed rather than the WT (Bayascas et al., 2006; Tahimic et al., 2013). These three methods have given investigator great flexibility in constructing conditional alleles.

Once a conditional gene targeting system has been integrated and validated in a mouse genome, the investigator must decide how and when to 'switch on' the mutation. To switch on a Cre/*loxP* conditional mutation requires two reagents, typically in the form of two different GM mouse lines. One mouse line expresses the Cre recombinase under the control of a cell specific or developmental specific promoter. The other line carries the conditional allele. After crossing the

two GM mouse lines, cells expressing Cre recombinase in the offspring will recombine the *loxP* sites and switch on the mutation (Bayascas et al., 2006). An alternative method for temporally controlling conditional alleles is to introduce a tamoxifen-inducible Cre recombinase allele into the conditional mouse model. Using this strategy, Cre recombinase is not expressed until tamoxifen is applied topically or by injection into the mouse (Bayascas et al., 2006; Tahimic et al., 2013). By controlling when and where mutations are activated in a mouse model enables investigators to study the mechanistic consequences of genetic alterations in a particular tissue and/or at a specific stage of development.

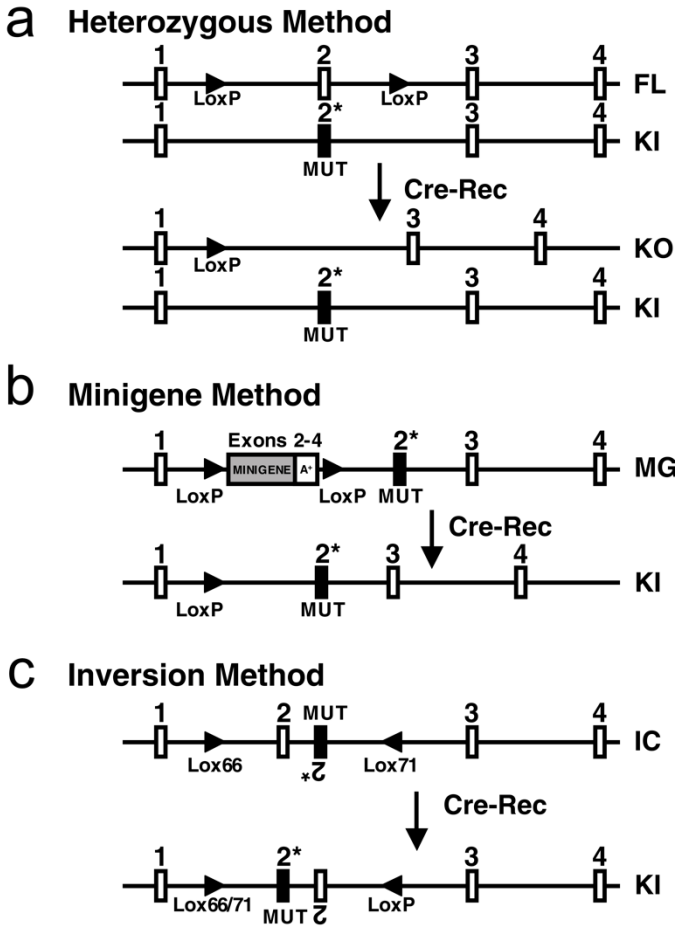

Figure 1.6 Conditional knock in (KI) strategies: (a) heterozygous method, (b) minigene method and (c) inversion method. A hypothetical gene consisting of four exons is depicted. The white boxes are wild type (WT) exons and the black boxes represent a mutant exon 2. The black arrows indicate the orientation of *loxP* sites. The minigene (MG) cassette is depicted as a gray box and corresponds to WT exons 2– 4 followed by a polyadenylation transcription termination signal (A). Cre-Rec is Cre-mediated recombination. IC is inversion cassette. Image modified and adapted from Bayascas et al. (2006).

1.7 Aim

This study aims to generate a GM mouse model with a conditional KI missense point mutation in the F-box and WD40 repeat domain-containing 7 gene (Fbxw7). Fbxw7 has pivotal roles in cell division, growth, and differentiation by degrading several proteins, including c-Myc, Notch1, Notch4, c-Jun, and cyclin E (Nakayama & Nakayama, 2006). Given that most of these proteins targeted by Fbxw7 for degradation are proto-oncoproteins, Fbxw7 has been proposed to function as a tumour suppressor gene (Davis et al., 2014; Davis et al., 2011). Indeed, Fbxw7 is commonly mutated in a diverse range of tumors, including colorectal, breast and lung cancer. In a previous study, the conditional deletion of both alleles of *Fbxw7* in the intestine of mice was shown to induce the development of adenomas that accumulate several Fbxw7 substrates, including both c-Myc and Notch1 (Babaei-Jadidi et al., 2011). As existing mutant Fbxw7 mouse models carry null alleles, this study aims to create a mouse model carrying one of the commonly occurring point mutations in human cancers (Fbxw7(R482Q); Davis et al., 2011). Fbxw7(R482Q) is a guanine to adenine mutation within exon 12 that results in an arginine to glutamine substitution in the substrate recognition domain of Fbxw7.

To generate the $Fbxw7^{R482Q}$ mouse model, a CRISPR/Cas9-assited gene targeting strategy will be employed to generate mESC clones harboring a 5.5 kb Cre-dependent conditional KI construct. The KI construct contains a floxed WT Fbxw7 minigene and STOP cassette followed by the Fbxw7(R482Q) mutant allele and cyan fluorescent protein (CFP) reporter gene. The system allows for Cre-dependent conditional expression of the Fbxw7(R482Q) mutant allele and CFP from the natural promoter. By including a CFP reporter gene it permits investigators to visually identify cells expressing of the mutant Fbxw7(R482Q) allele. Confirmed mESC clones will be injected into WT blastocysts to develop into chimeric mice for further breeding. In developing the $Fbxw7^{R482Q}$ mouse model, this reported will highlight key methodologies and findings for generating conditional KI alleles using CRISPR/Cas9 in mESCs. Methods and findings will include: gRNA design and validation, subcloning of gRNA into a CRISPR expression plasmid, the transfection and screening of mESCs, functional testing of Cre-dependent conditional KI alleles, blastocyst microinjection and uterine transfer, and finally discuss future breeding plans for germline competent chimeras. Once a breeding population is established the $Fbxw7^{R482Q}$ mouse

model will be used by the Tomlinson group at the Wellcome Trust Centre for Human Genetics (WTCHG) to study the role of the Fbxw7(R482Q) in the development of colorectal cancer.

2 Materials

2.1 Buffers and solutions

1% agarose gel

Components	Amount	Company
Agarose	1.5g	Sigma-Aldrich, US
Ethidium Bromide	3µl	Sigma-Aldrich, US
TAE (1X)	150ml	Severn Biotech, UK

PCR reaction mix (20µl)

Components	Amount	Company
Buffer (10x)	2µl	Bioline, UK
$MgCl_2$ (10µM)	0.6µl	Bioline, UK
Primer 1 (10µM)	1µl	Invitrogen, US Sigma-Aldrich, US
Primer 2 (10µM)	1µl	Invitrogen, US Sigma-Aldrich, US
dNTPs (10µM)	0.4µl	Bioline, UK
Taq Polymerase	0.2µl	Bioline, UK
Q Solution	4µl	Qiagen, GE
dH_2O	9.8µl	WTCHG, UK
Genomic DNA	1µl	N/A

Long Amplification PCR reaction mix (20µl)

Components	Amount	Company
Buffer (10x)	4µl	New England Biolabs, US
Primer 1 (10µM)	0.8µl	Invitrogen, US Sigma-Aldrich, US
Primer 2 (10µM)	0.8µl	Invitrogen, US Sigma-Aldrich, US
dNTPs (10µM)	0.6µl	WTCHG, UK
Long Amp. Taq. Pol.	0.7µl	New England Biolabs, US
dH20	12.1µl	WTCHG, UK
Genomic DNA	1µl	N/A

0.1% TE buffer

Components	Amount	Company
Tris HCl pH7.4 (1M)	100µl	Sigma-Aldrich, US
EDTA (0.5M)	20µl	Sigma-Aldrich, US
dH2O	99.7ml	WTCHG, UK

Additional buffers and solutions

Buffers and solutions	Company
Gel loading dye (6x)	New England Biolabs, US
Gel ladders (100bp and 1kb)	New England Biolabs, US
BbsI enzyme	New England Biolabs, US
T4 DNA Ligase	New England Biolabs, US
T4 Ligase Buffer	New England Biolabs, US
ATP 10mM	WTCHG, UK
Plasmid safe ATP dependent nuclease	Epicentre, US
Cutsmart buffer	New England Biolabs, US
Lithium chloride (8M)	Sigma-Aldrich, US
Isopropanol	Sigma-Aldrich, US
Ethanol	Sigma-Aldrich, US
Hind III - HF	New England Biolabs, US

2.2 Bacteria and cell culture media and reagents

Melanoma cell culture media

Components	Amount	Company
IMEM	45ml	Sigma-Aldrich, US
FCS	5ml	Thermo Fisher, US
L-glutamine (200mM)	1ml	Sigma-Aldrich, US
With penicillin/streptomycin selection:		
Penicillin/Streptomycin (10,000 U/ml)	500µl in 50ml of B16F10 media	Gibco, US

Embryonic stem cell (mESC) culture media

Components	Amount	Company
KnockOut DMEM (1X)	500ml	Thermo Fisher, US
FCS	50ml	Thermo Fisher, US
Penicillin/Streptomycin (10,000 U/ml)	6ml	Gibco, US
MEM Non-essential Amino acids (100x)	6ml	Sigma-Aldrich, US
1000x βME	500µl	Sigma-Aldrich, US
LIF	60µl	Millipore, UK
With puromycin selection:		
Puromycin (1mg/µl)	30µl in 50ml of JM8 media	Sigma-Aldrich, US
With neomycin selection:		
G418 (350ng/µl)	30µl in 50ml of JM8 media	Sigma-Aldrich, US
With neomycin half selection:		
G418 (350ng/µl)	15µl in 50ml of JM8 media	Sigma-Aldrich, US

Trypsin 2X + G

Components	Amount	Company
EDTA (0.5M)	0.1g	Sigma-Aldrich, US
D-Glucose	0.5g	Sigma-Aldrich, US
Chicken Serum	5ml	Thermo Fisher, US
Trypsin (2.5%)	20ml	Thermo Fisher, US

Freezing media for embryonic stem cells

Components	Percentage	Company
JM8 ES cell media	40%	WTCHG, UK
FCS	40%	Thermo Fisher, US
DMSO	20%	Sigma-Aldrich, US

Lysis buffer for cell culture

Components	Amount	Company
SDS (0.1%)	1ml	Sigma-Aldrich, US
Proteinase K (20mg/ml)	20µl	Bioline, UK
RNase A (10mg/ml)	4µl	Sigma-Aldrich, US

Additional reagents

Reagents	Company
Chorionic gonadotropin human (hCG)	Sigma-Aldrich, US
Dulbecco's phosphate buffered saline	Sigma-Aldrich, US
Fugene HD Transfection Reagent	Promega, US
KSOM	Thermo Fisher, US
LB Agar	Sigma-Aldrich, US
LB Broth	Sigma-Aldrich, US
M2 media with HEPES	Sigma-Aldrich, US
Opti-MEM	Thermo Fisher, US
Pregnant mare's serum gonadotropin (PMSG)	Sigma-Aldrich, US
Purified mineral oil	Sigma-Aldrich, US
TAT-Cre Recombinase (207uM)	Millipore, UK
Trypsin-EDTA	Sigma-Aldrich, US
Vetergesic (buprenorphine)	Sogeval, UK
Water for embryo transfer	Sigma-Aldrich, US

2.3 Bacteria, cells and animals

Bacteria	Company
ElectroSHOX Escherichia coli	Bioline, US

Murine cell line	Common name
JM8.F6 male embryonic stem cells	Mouse embryonic stem cells (mESCs)
B16F10 melanocytes	Mouse melanoma cells
DR4 Murine embryonic fibroblasts	Murine embryonic fibroblasts (MEFs)

Mouse strain	Common name	Utility
B6(Cg)-Tyrc-2J/J	Bl6-Albino	Blastocyst harvesting Chimeric breeding program
CD1	CD1	Foster mothers

2.4 Primers

gRNA primers were designed using the CRISPOR online tool (http://crispor.tefor.net), which was developed by Haeussler et al. (2016). Critically, a gRNA was selected with a target site present in the natural WT Fbxw7 allele but absent in the donor DNA plasmid (Fbxw7 donor plasmid). Overhangs were added to the gRNA primers to accommodate for BbsI restriction sites that were used for ligating the annealed gRNA primers into the CRISPR expression plasmid. BbsI specific overhangs are shown below in red on annealed gRNA primers.

```
CRISPR primer forward: 5'-CACCGGGACCCTGGTTCCACCTCA-3'
CRISPR primer reserve:     3'-CCCTGGGACCAAGGTGGAGTCAAA-5'
```

All other primers were designed using Primer3 (version 0.4.0) software. All primers were purchased from either Invitrogen or Sigma-Aldrich. Working concentrations for all primers was 10μM.

gRNA primers

Primer	Orientation	Sequence
gRNA-F	Forward	5'-CACCGGGACCCTGGTTCCACCTCA-3'
gRNA-R	Reverse	3'-AAACTGAGGTGGAACCAGGGTCCC-5'

Primers for sequencing

Primer	Orientation	Sequence
U6-F	Forward	5'-AATCATGGGAAATAGCCTC-3'
Fbxw7-F	Forward	5'-TGAGCACGTGTCTGAAACTGA-3'

Primers for screening mutagenesis

Primer pair (PP)	Orientation	Sequence
PP1	Forward	5'-TGAGCACGTGTCTGAAACTGA-3'
	Reverse	5'-GTAAACACTGGCCGGTCTCA-3'
PP2	Forward	5'-TAGGCATAATATTGAGGATGGAAGC-3'
	Reverse	5'-TGGTCATGTCCACTATGGACTC-3'
PP3	Forward	5'-GGAGAGCTGTGGTATGTGGC-3'
	Reverse	5'-CCTTGATGCCATTCTTCTGC-3'

2.5 Plasmids

This section lists all plasmids used in this study. An overview of the functional features within each plasmid can be found in Appendix A. The concentration and quality of the plasmid purifications are shown in the NanoDrop™ spectrophotometry readings in Appendix B.

2.5.1 CRISPR expression plasmid

The CRISPR expression plasmid was purchased from the Addgene repository, where its official name is pX330-U6-Chimeric_BB-CBh-hSpCas9 (Plasmid #42230). It is a human codon-optimized SpCas9 and gRNA expression plasmid. The plasmid was initially designed by Cong et al. (2013) and was a gift to the Addgene repository from Dr Feng Zhang. After acquiring the plasmid, Dr Ben Davies at WTCHG modified the plasmid by adding a puromycin resistance cassette.

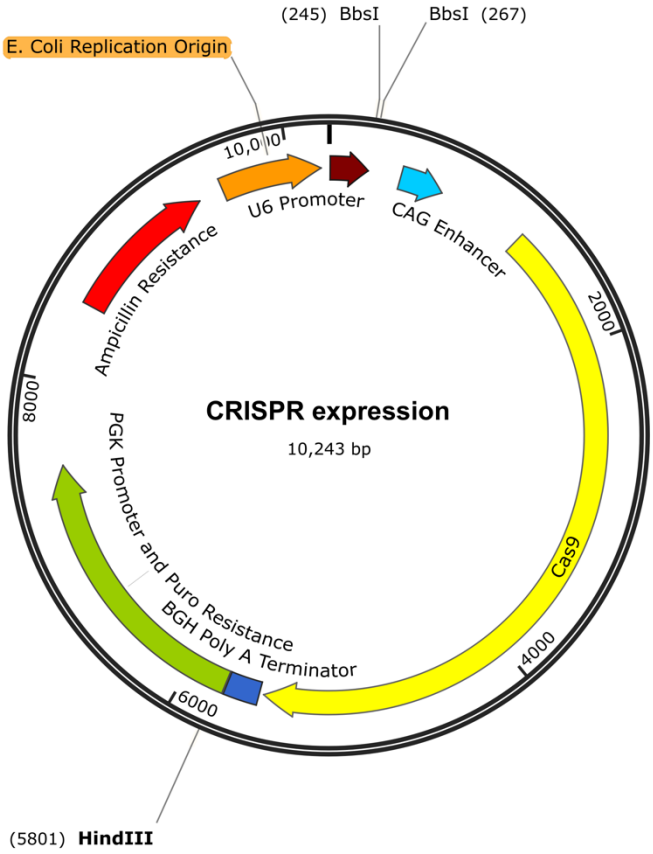

Figure 2.1 CRISPR expression plasmid map (map was modified and adapted from addgene.org). The functional role of each plasmid feature is described in Appendix A.

2.5.2 Fbxw7 donor plasmid

The Fbxw7 donor plasmid was designed and constructed by the Tomlinson group at the WTCHG. The official name of the plasmid is pMA-mFbxw7(R482Q)-CFP. It is a donor DNA plasmid targeted at inserting Cre-dependent conditional KI point mutation (R482Q) within intron 11 of Fbxw7. The missense point mutation (R482Q) is within exon 12. A CFP reporter gene is included to tract expression of the mutant Fbxw7(R482Q) allele. The plasmid also has carries neomycin resistance gene for positive selection and diphtheria toxin A cassette for negative selection.

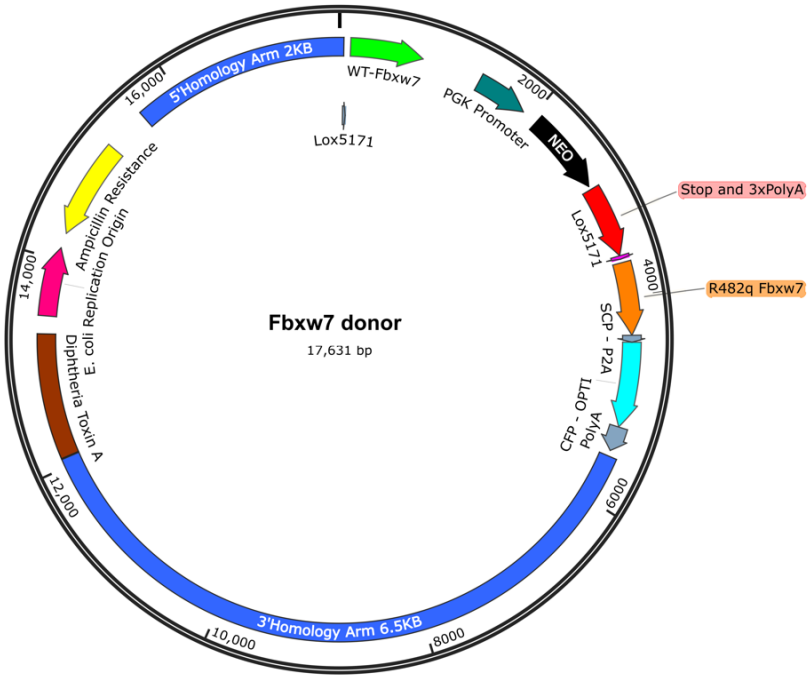

Figure 2.2 Fbxw7 donor plasmid map (map was sourced from the Tomlinson group at the WTCHG). The functional role of each plasmid feature is described in Appendix A.

2.5.3 GFP expression plasmid

The green fluorescent protein (GFP) expression plasmid was constructed by Dr Ben Davies at the WTCHG. The official name of the plasmid is pCX-eGFP. It is frequently used as a control to assess plasmid transfection efficiency in mammalian cells. It sole role is to express GFP.

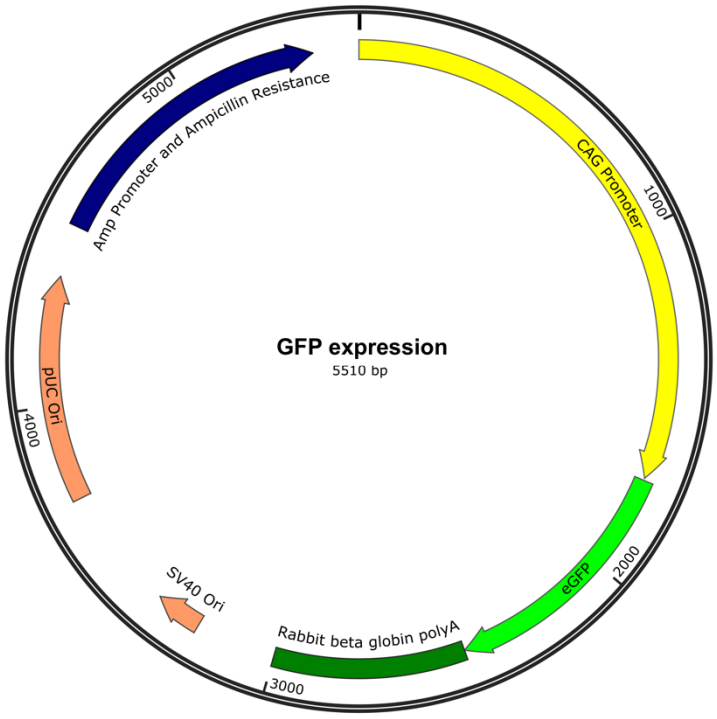

Figure 2.3 GFP expression plasmid map (map was sourced from Dr Ben Davies at the WTCHG). The functional role of each plasmid feature is described in Appendix A.

2.6 Kits

Kit	Company
GeneJET Plasmid Midiprep Kit	Thermo Fisher, US
Mix2Seq Kit	Eurofins, GE
Neon Transfection Kit	Invitrogen, US

2.7 Software

Software	Company
CRISPOR	Tefor Infrastructure, FRA
Endnote X7	Thomson Reuters, US
Microsoft Office	Microsoft, US
SnapGene	GSL Biotech LLC, US
TIDE analysis	Netherlands Cancer Institute, NE
USCS Genome Browser	University of California, US

2.8 Equipment and consumables

Equipment and consumables	Company
Cell imaging system	Biorad, US
Centrifuge and PCR tubes	VMR, US
Centrifuges	Thermo Fisher, US
Electrophoresis gel chambers	Hoefer, US
Gel imaging system	Biorad, US
Heating block	Jencons, US
Incubator	New Brunswick, GE
Micromanipulator	Eppendorf, GE
Microscope	Nikon, JAP
Mr Frosty Freezing Container	Thermo Fisher, US
NanoDrop™ spectrophotometer	Thermo Fisher, US
Neon electroporation system	Invitrogen, US
Pipettes	Gilson, US
Thermocycler	VWR, US
Thermomixer	Eppendorf, GE
Tissue culture plates and flasks	Cellstar, US
Vortex	Scientific Industries, US

3 Methods

3.1 Molecular biology techniques

3.1.1 Annealing gRNA primers

To anneal the gRNA primers, the reagents listed below were added to a 1.5ml microcentrifuge tube and incubated at 100°C for 5 mins in a heating block. The heating block was then turned off and tubes were left to cool to room temperature in the heating block.

Reagents	Volume (µl)
gRNA-F primer (100µM)	2
gRNA-R primer (100µM)	2
TE Buffer pH 8.0 (0.1%)	16

3.1.2 Subcloning of gRNA primers into CRISPR expression plasmid

The annealed gRNA primers were subcloned into the CRISPR expression plasmid using Bbsi restriction sites (Figure 4.2). All reagents listed below were added to a 0.2ml PCR tube.

Reagents	Volume (µl)
CRISPR expression plasmid (150ng/µl)	1
Annealed gRNA Primers	1
BbsI	1
T4 DNA ligase	1
T4 Ligase Buffer (10x)	2
dH2O	14

The mixture was then and run on a thermocycler with the following parameters.

Step	Temperature	Time (mins)
1	37°C	5
2	16°C	10
	Repeat steps 1 through 2 for 9 additional cycles	
4	50°C	5
5	80°C	5
6	4°C	Infinite

Once the reaction had cooled to 4°C the mixture was treated with plasmid safe nuclease by adding the reagents listed below into the 0.2ml PCR tube. The mixture was then incubated in a thermocycler at 37°C for 1 hour before storing at -20°C until required.

Reagents	Volume (µl)
Cloned CRISPR expression plasmid plasmid	20
10mM ATP	1
Plasmid Safe Nuclease	1

3.1.3 Amplification and purification of CRISPR expression plasmid

To amplify the cloned CRISPR (cCRISPR) expression plasmid, 500ng of cCRISPR expression plasmid was added to 100µl of ElectroSHOX *E. coli* in 1.5ml microcentrifuge tube. After 20 mins on ice, the tube was heat shocked at 42°C for 90 secs and immediately placed back on ice for a further 5 mins. The culture was then plated onto a 10cm LB agar plate with 100mg/ml of ampicillin and grown for 24 hours at 37°C. The following day one isolated bacterial colon was picked into 50ml LB broth with 100mg/ml ampicillin and incubated overnight at 37°C on a rocking platform. The plasmid was then extracted and purified using GeneJET Plasmid Midiprep Kit following the manufacturer's instructions.

3.1.4 Validated cCRISPR expression plasmid

Two assays were undertaken to confirm successful subcloning of the annealed gRNA primers into the cCRISPR plasmid. Firstly, 2µl of the purified cCRISPR plasmid was digested with BbsI and HindIII restriction enzymes. The plasmid digest was then run on a 1% agarose gel electrophoresis (GE) and imaged. Secondly, the cCRISPR plasmid was sent for Sanger sequencing using the U6-F primer.

3.1.5 Lysis and DNA extraction from cells

Confluent cells were lysed with Lysis Buffer for cell culture using an appropriate amount for plate size and incubated at 37°C for 16 hours. Lithium chloride and isopropanol DNA purification was then performed on the lysate. $1/10^{th}$ volume of lithium chloride (8M) and 1 volume of isopropanol were added to the plate and placed on a rocking platform for 20 mins. The plate was the centrifuged

at 2500rpm for 20 mins and the supernatant discarded. The plate was the washed twice with 70% ethanol and the resulting DNA pellet was resuspended in an appropriate amount of 0.1% TE buffer.

3.1.6 PCR protocols

PCR products of <1000bp were amplified using the PCR protocol shown below. The lid temperature of the thermocycler was set at 111°C.

Step	Temperature	Time
1	95°C	10 mins (hot start)
2	94°C	1 mins
3	57°C	1 mins
4	72°C	30 secs
	Repeat steps 2 through 4 for 31 additional cycles	
5	72°C	10 mins
6	4°C	Infinite

PCR products of >1000bp were amplified using the PCR protocol shown below. The lid temperature of the thermocycler was set at 112°C.

Step	Temperature	Time
1	94°C	2 mins 30 secs (hot start)
2	94°C	30 secs
3	60°C	40 secs
4	65°C	50 secs per 1000bp
	Repeat steps 2 through 4 for 31 additional cycles	
5	65°C	10 mins
6	4°C	Infinite

3.1.7 DNA gel electrophoresis

All PCR products <1000bp were run in 2% agarose gel made from 1% TAE, whilst products >1000bp were run in 1% agarose gel made with 1% TAE. Gel chambers were filled with 1% TAE buffer and operated at 120V and 300mA. Time varied appropriate to the size of PCR product and resolution required.

3.1.8 Sanger sequencing

All Sanger sequencing was performed by Eurofins Germany using their Mix2Seq kit and following the company's preparation guidelines.

3.2 Cell culture protocols

All cells were cultured at 37°C with 5% CO_2. Culture media was refreshed daily. A workflow of both the melanocyte and mESC culturing procedures used in this study can be found in Appendix C.

3.2.1 Mouse melanoma cell culture

B16F10 melanoma cells were thawed and expanded in melanoma cell culture media with penicillin/streptomycin up to a T25 culture flask. Passaging of melanoma cells involved washing twice with PBS before adding Trypsin-EDTA and incubating for 5 mins at 37°C. Trypsin was then neutralised with an appropriate amount of cell culture media.

Lipofection of melanoma cells

At 70% confluence, media was changed to melanoma cell culture media with no penicillin/streptomycin in preparation for lipofection. For lipofection, 550ng of cCRISPR expression plasmid was mixed with 26µl of Opti-MEM media and 1.7µl of Fugene HD reagent in a 1.5ml microcentrifuge tube. The mixture was then incubated at room temperature for 10 mins. 550ng of GFP expression plasmid was prepared in identical fashion. 25µl of each incubated complex was added to separate wells in 24 well plate (WP) with 70% confluent melanoma cells. Cells were then incubated for 24 hours before changing back to melanoma cell culture media with penicillin/streptomycin.

Analysis of transfected melanoma cells

Once confluent, melanoma cells lipofected with GFP expression plasmid were assessed for GFP expression under fluorescence microscopy using a fluorescein isothiocyanate (FITC) filter. Cells

transfected with cCRISPR expression plasmid and the non-transfected control melanoma cells were lysed and DNA was extracted. Extracted DNA was PCR amplified across the CRISPR/Cas9 target site using primer pair 1 (PP1). The PCR product were sent for Sanger sequencing using PP1-Forward primer. A tracking of indels by decomposition (TIDE) analysis was then undertaken using the quantitative trace data from the two Sanger sequencing reactions. The TIDE analysis was performed using the Netherlands Cancer Institute TIDE analysis web tool (http://tide-calculator.nki.nl) with default settings. This free online tool was developed by Brinkman et al. (2014).

3.2.2 Embryonic stem cell culture

JM8.F6 mESCs were thawed and expanded in ESC culture media on MEF feeder layer up to T75 culture flask. Passaging of mESCs involved aspirating off media and washing twice with PBS before adding trypsin 2X+G and incubating for 8 mins at 37°C. Trypsin was then neutralised with an appropriate amount of cell culture media.

Electroporation of embryonic stem cell

In preparation for electroporation, mESCs in T75 flask were passaged and resuspended at 1 x 10^6 cells per 100µl in Buffer R from the Neon Transfection Kit. 100µl of mESC suspension and 5ug of both cCRISPR expression plasmid and Fbxw7 donor plasmids were mixed in a 1.5ml microcentrifuge tube. Using the Neon electroporation system with settings 1400V, 10ms and 3 pulses, the cells and plasmid mixture were electroporated. The electroporated suspension was then dispersed over a 10cm culture plate prepared with MEFs and mESC culture media. After 24 hours, positive selection began with 48 hours exposure to puromycin. After 48 hours in puromycin selection the cells were changed to neomycin selection. Cells were left in neomycin selection until 70% confluent and ready for picking.

Picking transfected embryonic stem cell colonies

After selection, single healthy mESC colonies were picked. The term ‘picked’ means to you remove a single colony with as little MEFs as possible. Colonies were picked using 20µl filter pipette tip set to 10µl under phase microscope and transferred into 96 WP holding 30µl of trypsin

in each well. After picking, the 96WP was incubated for 5 mins at 37°C before neutralising the trypsin by adding 70µl of mESC culture media into each well. Picked colonies in the 96WP were then resuspened by pippeting up and down and transferred to a 96WP lined prepared with MEFs and 100µl of mESC culture media in each well. After 24 hours the media in the 96WP was changed to neomycin half selection.

1:3 splitting of a 96 well plate

Once picked mESC clones became confluent the 96WP was split into three 96WPs. Media was removed from the original 96WP and washed twice with PBS. 30µl of trypsin 2X+G was added to each well and incubated for 8 mins before neutralizing with 150ul of mESC culture media. Three 96WPs were then prepared to collect the cells. 150µl of mESC culture media was added to each well in two 96WPs lined with MEFs and one 96WP lined with 0.1% gelatin. Once the collection plates were prepared, 60µl of the 180µl of cell suspension was split into each well of the three 96WPs. After 24 hours, the media was changed to neomycin half selection.

Freezing a 96 well plate

To freeze a 96WP, the media was aspirated off and wells washed twice with 150µl of PBS. 30ul of trypsin 2X+G was then added to each well and incubated for 8 mins. The tryspsin was then neutralised with 70µl of cell culture media. 100µl of Freeze mix was then added to each well. Each well was covered with 50µl of mineral oil. The plate was sealed with parafilm and placed into a Styrofoam box layered with wet ice. The box was then stored at -80°C.

Freezing cyrovials of positive clones

Media was aspirated off cells in the culture flask and cells were washed twice with a suitable amount of PBS. Trypsin 2X+G was added and incubated for 8 mins at 37°C before neutralizing with mESC culture media. Cells were then resuspend before centrifuging for 5 mins at 1000rpm. The supernatant was aspirated off and the pellet of cells was resuspended in mESC culture media (250µl per cyrovial). To each cryovial 250µl of freeze mix and 250µl of the cell suspension was added. Cyrovials were placed into ‘Mr Frosty’ freezing vessel and stored at -80°C.

Thawing positive clones from 96 well plate

A 24WP with MEF feeder layer was prepared with 1ml of prewarmed mESC culture media. The 96WP was thawed inside a waterproof bag in a 37°C water bath. Once thawed, a 200µl pipette, set to 180µl was plunged into the well of the confirmed clone to be thawed. With the tip of the pipette below the mineral oil, the cells were extracted. The entire 180µl was transferred into the prepared 24WP and cultured until ready to passage.

Thawing positive clones from cyrovials

The cryovial was quickly thawed in a 37°C water bath. Once a small piece of ice was visible, 0.5ml of prewarmed mESC cell culture media was added to complete the thaw. The entire contents of the thawed cryovial was added to a 15ml falcon tube, along with an additional 4ml of mESC cell culture media. The falcon tube was centrifuged at 1000rpm for 5 mins. The supernatant was discarded and cell pellet was resuspended in a suitable volume of media for the intended purpose.

TAT-Cre recombinase treatment of embryonic stem cell

Once positive clones in 96WP reached 40% confluence the media was refreshed and 6µM of TAT-Cre recombinase was added to each well. The plate was incubated overnight before aspirating off the TAT-Cre containing media and replacing with fresh mESC culture media.

3.3 Mouse and embryo procedures

The care and maintenance of all mice used in this study was undertaken by trained animal technicians at the WTCHG. All of the procedures described in this section were performed by trained transgenic technologist in accordance with the UK Home Office Animals (Scientific Procedures) Act 1986 and the University of Oxford ethics committee. The methodologies described in this section are intended to provide a concise overview. For further details, please refer to ‘Manipulating the Mouse Embryo’ by Behringer et al. (2014).

3.3.1 Superovulation

In preparation for blastocyst harvesting, Bl6-albino females were superovulated by injecting each mouse with 3.75 IU of pregnant mare's serum gonadotropin (PMSG) followed by the same dose of human chorionic gonadotropin (hCG) 46 to 48 hours later. Both hormones were administered by intraperitoneal injection with a 25 gauge syringe. After administration of hCG, each female was placed into a cage with one stud male. The following morning, superovulated females were checked for vaginal plugs.

3.3.2 Mouse culling protocol

Mice were culled by cervical dislocation when required. Their necks were humanely broken by quickly applying firm pressure at the base of the skull, while at the same time pulling the tail backwards.

3.3.3 Blastocyst harvesting

Superovulated and plugged females were left for 2.5 days post cortium before culling. The abdominal cavity was immediately opened and the reproductive organs located. A cut was then made between the oviduct and the ovary, keeping the uterotubal junction intact. The uterus was removed and placed into M2 media with HEPES. Blastocysts were then flushed through the infundibulum and collected using an embryo handling pipette. Blastocysts were rinsed and kept in KSOM media overnight at 37°C. The following day healthy blastocyst were microinjected with confirmed Fbxw7(R482Q) mESCs.

3.3.4 Blastocyst microinjection

‘Black coat’ Fbxw7(R482Q) confirmed mESCs were injected into ‘white coat’ Bl6-albino blastocysts. Successful integration of the black coat Fbxw7(R482Q) targeted mESCs will yield black and white chimeric pups. See Figure 3.1 for pictures from blastocyst microinjection process.

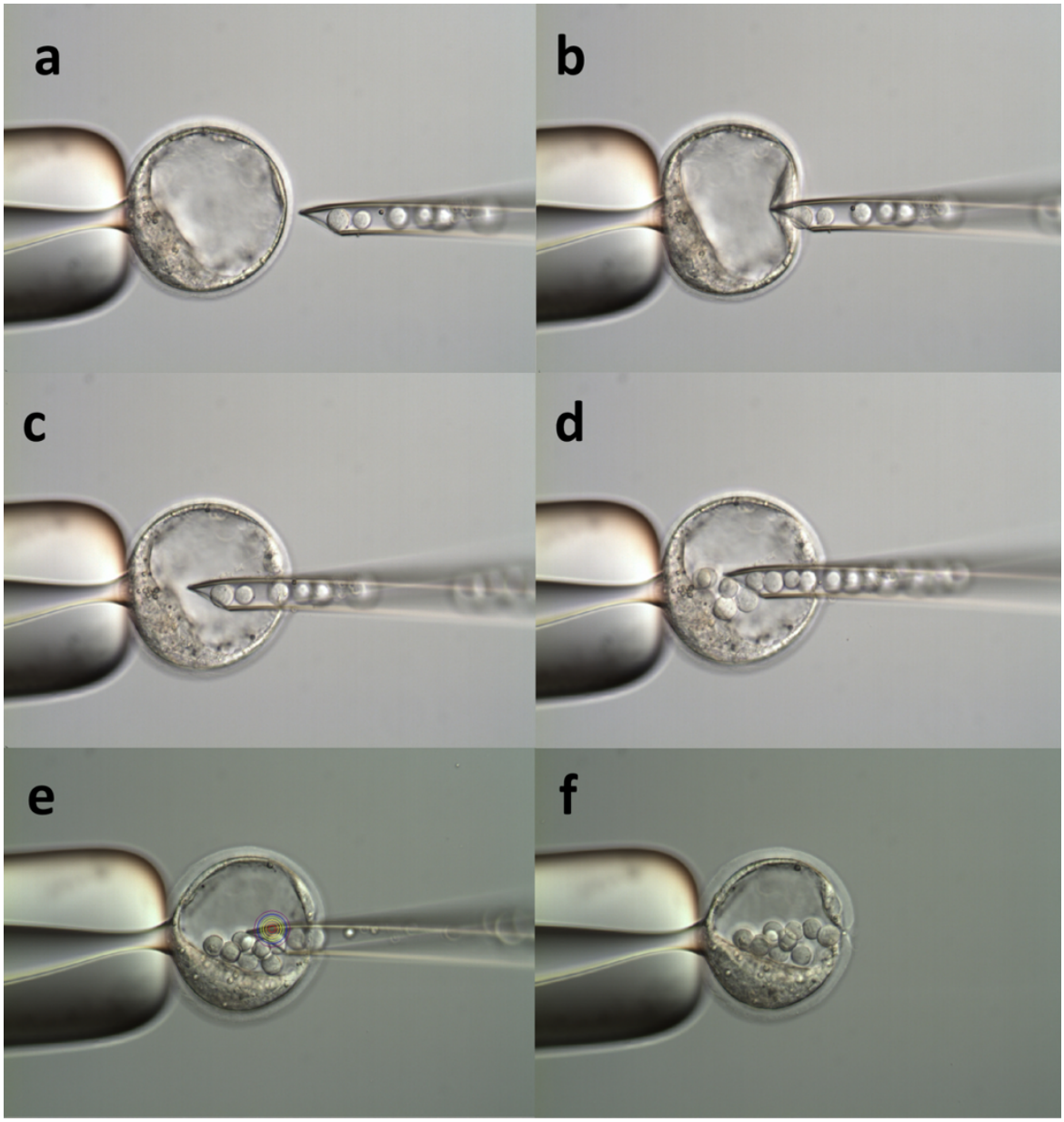

Figure 3.1 Blastocyst microinjection process. (a) The injection needle collects healthy and undifferentiated mouse embryonic stem cells (ESCs) and are positioned near the pipette tip. A blastocyst is then immobilised on a holding pipette so that the inner cell mass is at 6 o'clock. (b) and (c) The needle is gentle pushed into the blastocyst cavity. (d) and (e) 10 to 12 mESCs are slowly released into the blastocyst cavity. (f) The needle is slowly withdrawn and the blastocyst walls collapse back together.

3.3.5 Blastocyst uterine transfer

A CD1 pseudo pregnant foster mother was anesthetized with inhaled isoflourane at 4% for induction and 2% for maintenance. Oxygen flow was set between 400 to 500 ml per min. A transfer pipette was loaded with blastocysts previously injected with targeted mESCs. The foster mother was placed on her abdomen and a small 1 cm incision was made in her back. Through the incision the uterus was located and a small hole was made in the uterine wall using a 25 gauge needle. After removing the needle, the transfer pipette, loaded with the blastocysts was placed into the hole and approximately 15 blastocysts were expelled. The reproductive organs were then relocalised and the body wall sutured and wound clips added. Each foster mother was administered with buprenorphine to assist in relieving any post-surgical pain.

4 Results

4.1 gRNA design

The gRNA was designed using the CRISPOR online tool (Haeussler et al., 2016) and had the predicted characteristics shown in Table 4.1. It's important to note that the gRNA target site was not present in the Fbxw7 donor plasmid to prevent recurrent cleavage after HDR integration. The expected gRNA target site within the mouse genome (GRCm38/mm10) is depicted below in Figure 4.1.

Table 4.1 gRNA characteristics generated using CRISPOR online tool.

gRNA Primer (cDNA)	PAM	Specificity Score	Predicted efficiency	Off-targets for mismatches				
				0	1	2	3	4
5'-GGGACCCTGGTTCCACCTCA-3'	AGG	72	51	0	0	1	15	125

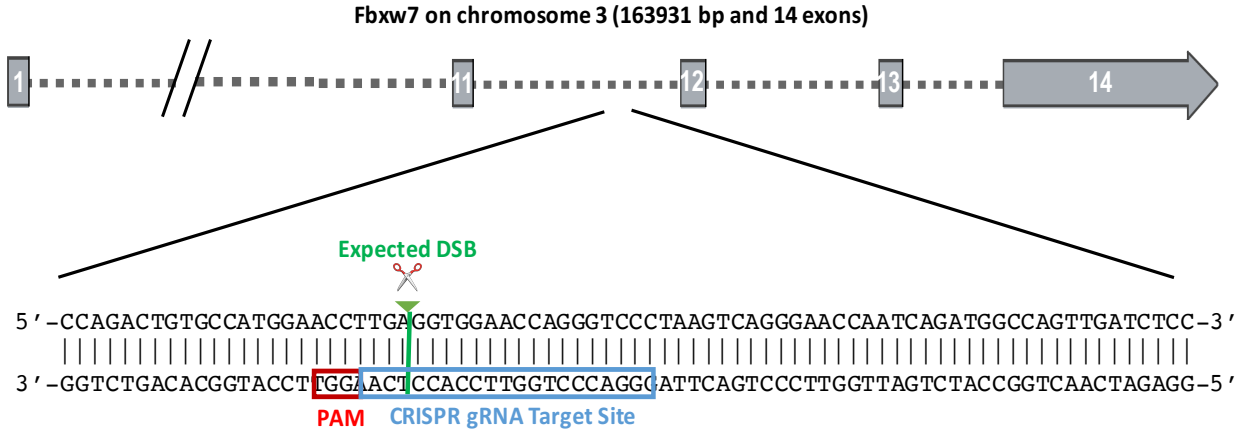

Figure 4.1 gRNA target site. The designed gRNA is expected to produce a double stranded DNA break (DSB) in intron 11 of Fbxw7 gene on chromosome 3 in the mouse genome.

4.2 Validation of cCRISPR expression plasmid

Annealed gRNA primers were subcloned into the CRISPR expression plasmid using BbsI restriction sites. A successful cloning protocol removes the BbsI recognition sites (Figure 4.2). To validate the cCRISPR expression plasmid, the plasmid was digested with BbsI and HindIII

restriction enzymes. The location of these restriction sites in the CRISPR expression plasmid can be seen in Figure 2.1. The plasmid digestion was run on a gel electrophoresis (GE) which offered preliminary validation of a successful cloning protocol (Figure 4.3). Confirmation of the annealed gRNA primers in the cCRISPR expression plasmid was obtained by Sanger sequencing (Figure 4.4).

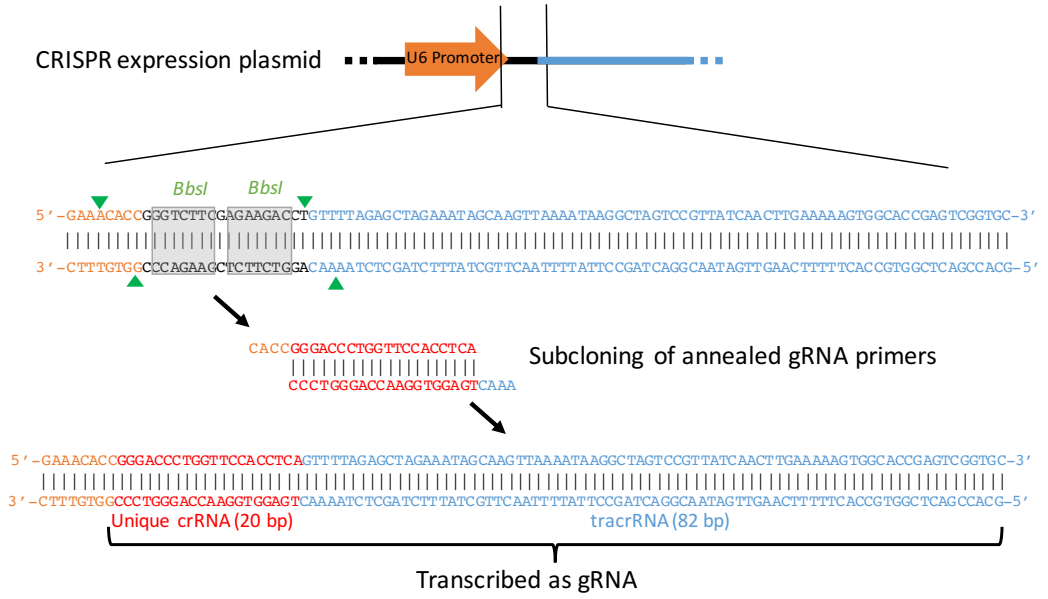

Figure 4.2 Cloning of annealed gRNA primers into BbsI restriction sites in CRISPR expression plasmid. Successful cloning disrupts BbsI recognition sites, which are highlighted in grey.

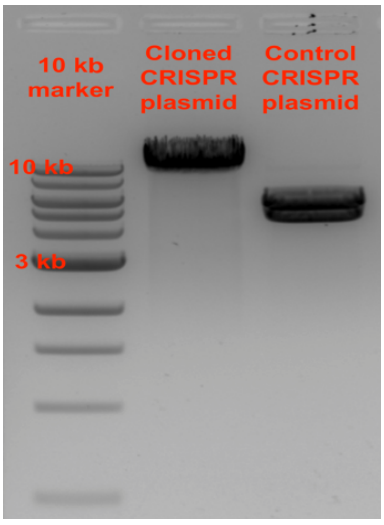

Figure 4.3 GE from digestion of CRISPR expression plasmids with BbsI and HindIII restriction enzymes. The control plasmid produced the predicted three bands at 22, 4687 and 5534 bp (22 bp band is not visible in this image). The cCRISPR expression plasmid produced only one band at 10243 bp, which indicates the removal of the BbsI recognition sites and successful integration of the annealed gRNA primers.

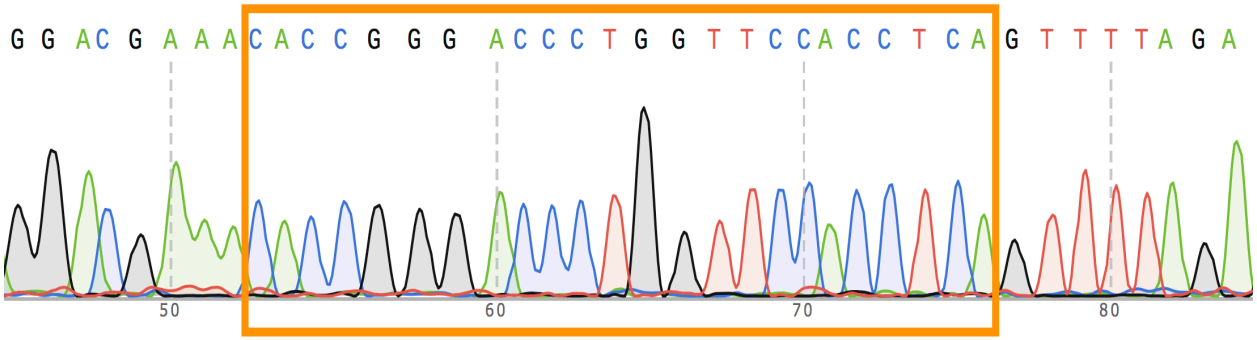

Figure 4.4 Sanger sequencing of cCRISPR expression plasmid confirmed the annealed gRNA primers had been successfully ligated into BbsI restriction sites. The integrated gRNA primer reads 5'-GGGACCCTGGTTCCACCTCA-3'.

4.3 Testing gRNA cutting efficiency in mouse melanoma cells

The gRNA cutting efficiency was tested in mouse melanoma cells. Cells were separately lipofected with cCRISPR expression plasmid and GFP expression plasmid. Cells lipofected with GFP expression plasmid were used to assess the transfection efficiency. Figure 4.5 illustrates the lipofection protocol was highly effective with numerous cells expressed GFP two days after transfection.

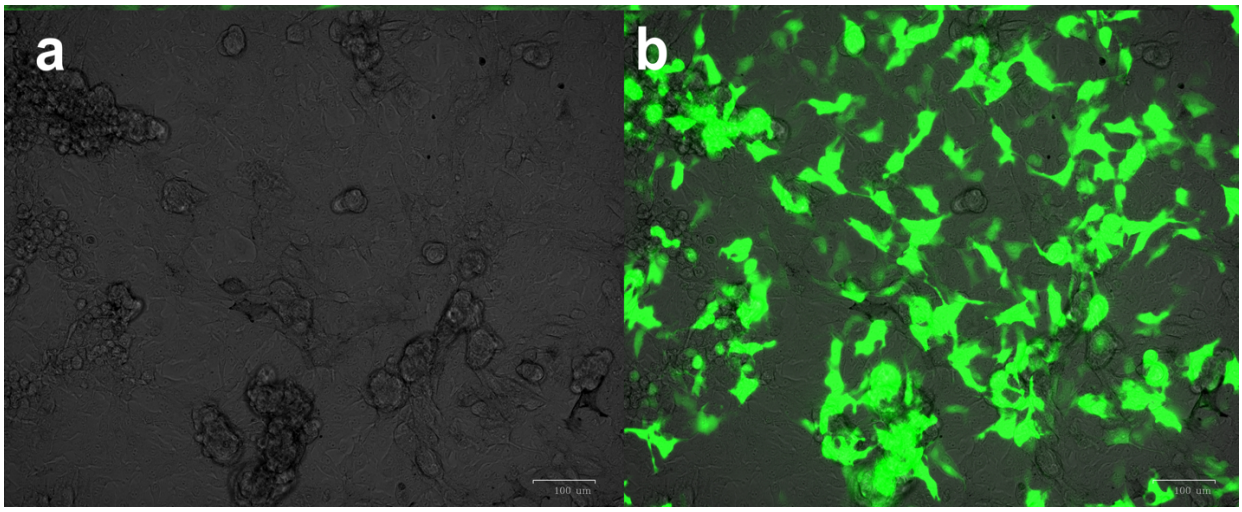

Figure 4.5 Mouse melanoma cells two days after lipofection with GFP expression plasmid. (a) Cells under phase microscopy. (b) Image 'a' merged with an image taken with fluorescein isothiocyanate (FITC) filter of the same field. Extensive expression of GFP indicates a successful lipofection protocol.

Mouse melanoma cells lipofected with the cCRISPR expression plasmid will express SpCas9 and the gRNA targeting the Fbxw7 locus (Figure 5.1). Once confluent, transfected cells were lysed and DNA extracted. The DNA from both targeted and control melanoma cells were separately sequenced across the gRNA target site. A TIDE analysis was performed using the qualitative sequence trace data from the two standard capillary sequencing reactions. The TIDE software calculated the total cutting efficiency of the gRNA to be 33.2% (Figure 4.7a). The efficacy of gRNA was further supported in the quality assurance graph depicted in Figure 4.7b. This graph illustrates that aberration of >20% between the control and Fbxw7 targeted sequences commences proximal (12 bp upstream) to the expected gRNA cut site.

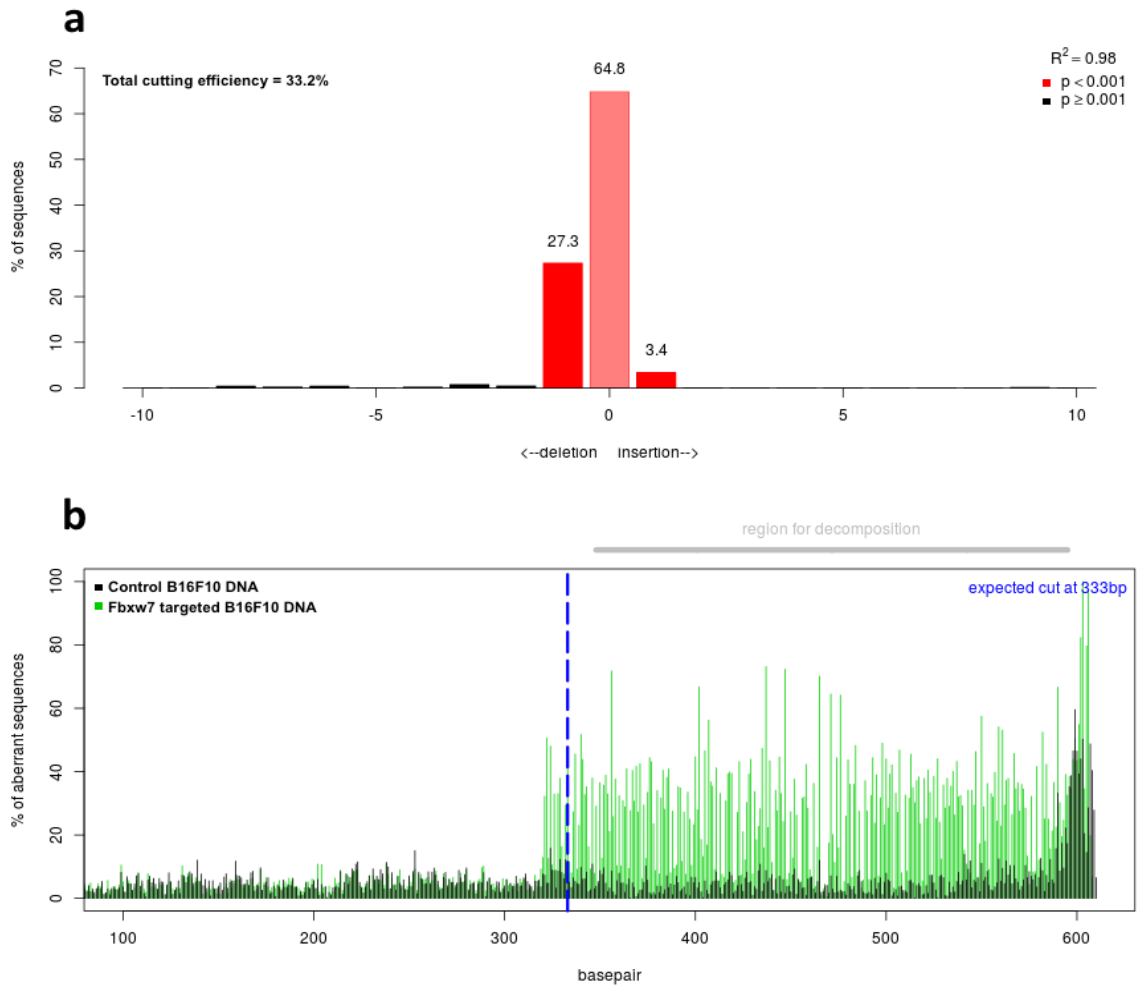

Figure 4.6 TIDE analysis results from gRNA testing in mouse melanoma cells. (a) The type and percentage of indels at gRNA target site. 27.3% of Fbxw7 targeted DNA had a 1 bp deletion, whilst 3.4% had a 1 bp insertion. The gRNA had a predicted cutting efficacy of 33.2%. (b) Aberrance between the control and Fbxw7 targeted sequences. Sequence aberration > 20% between the control and targeted DNA commences l2 bp upstream from expected gRNA cut site.

4.4 Screening of embryonic stem cells for positive clones

Sufficient cutting efficiency in mouse melanoma cells allowed the study to progress to gene targeting in mESCs. mESCs were electroporated with the cCRISPR expression plasmid and the Fbxw7 donor plasmid in an attempt to induce cellular repair of CRISPR-mediated DSBs via HDR. After selection, picking and expansion, 22 mESC clones remained that were screened for target vector integration via a series three PCRs. Figure 4.7 shows the expected PCR product sizes in positive clones using each of the three PCR primer pairs (PPs) employed.

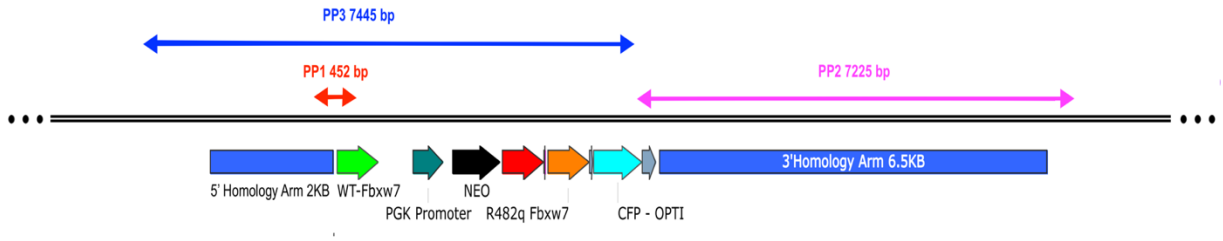

Figure 4.7 Screening for Fbxw7 construct integration. Expected PCR product sizes using primer pairs (PPs) 1, 2 and 3 in positive Fbxw7 targeted clones. PP1 (red), PP2 (pink) and PP3 (blue) have anticipated PCR product sizes in positive clones of 452, 7225 and 7445 bp, respectively.

4.4.1 Preliminary screening

Preliminary clone screening was performed using a PCR with PP1 to detect for the presence of the Fbxw7 construct. This screening provided no information on the genomic location of the donor construct. The variation between the PCR product sizes of the WT (640 bp) and the targeting construct (452 bp) was used to detect the presence of the Fbxw7 targeting construct (Figure 4.8). Of the 22 clones screened, 12 clones were preliminarily positive for construct integration and 9 clones were moved on for further screening (Figure 4.9). Furthermore, it should be noted that the absence or extremely weak WT signal in 5 of the 12 preliminarily positive clones is suggestive of a homozygous integration within those clones.

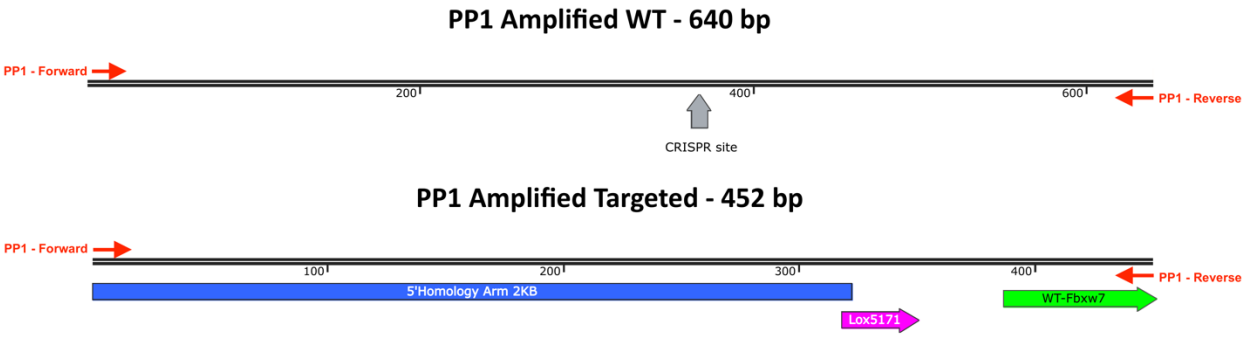

Figure 4.8 PCR product sizes of wild type clones (WT; 640 bp) and Fbxw7 targeted clones (452 bp) when amplified using primer pair 1 (PP1).

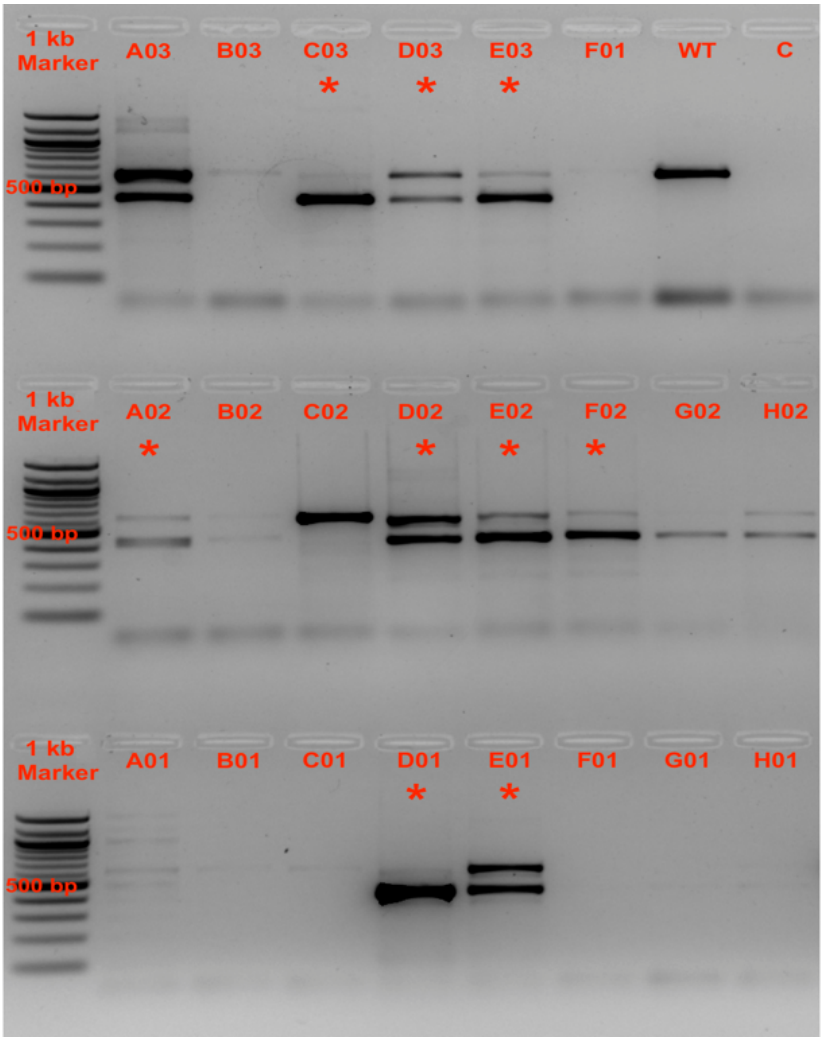

Figure 4.9 GE from preliminary PCR screening with primer pair 1 (PP1). Fbwx7 targeting construct produces a 452 bp band, whilst the wild type (WT) band is at 640 bp. Clones denoted with an asterisk were moved on for further screening. C is a water control.

4.4.2 Screening for 3' integration

A long range PCR was performed using PP2 to confirm 3' integration of the targeting construct in the 9 preliminary positive clones. Positive clones produce a PCR product of 7225 bp (Figure 4.10), whilst negative clones have no amplified PCR product. The results of the screening can be seen in the GE image in Figure 4.11. 6 of the 9 clones screened had strong positive bands at 7225 bp; however, for efficiency only 4 were progressed to the next stage of screening.

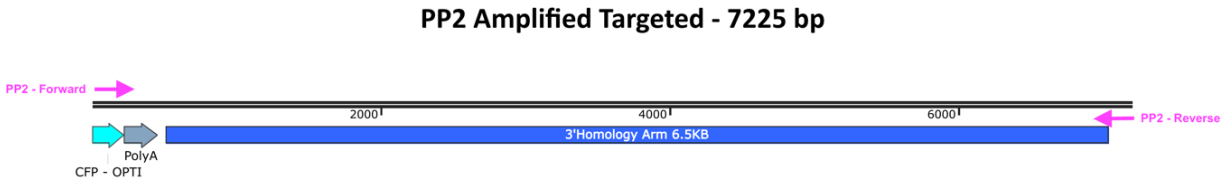

Figure 4.10. PCR product size in targeted clones with positive 3' construct integration using primer pair 2 (PP2). Positive clones will amplify a 7225 bp product and wild type clones will have no amplified PCR product.

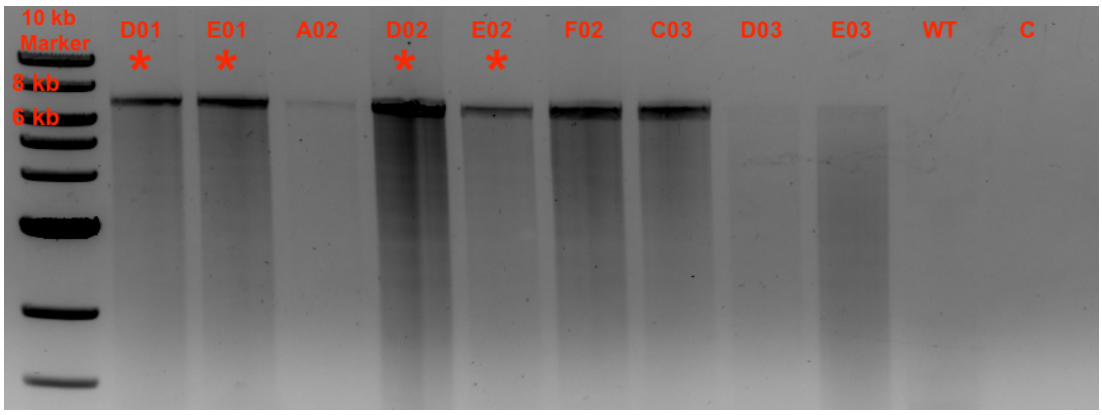

Figure 4.11 GE from PCR screening with primer pair 2 (PP2) to confirm 3' construct integration. Successful 3' integration produces a single band at 7225 bp. Wild type (WT) clones have no PCR product. Clones denoted with an asterisk were moved on for further screening. C is a water control.

4.4.3 Screening for 5' integration

To confirm 5' construct integration in the 4 putative positive mESC clones, a PCR was performed using PP3. Positive clones have a PCR product of 7445 bp (Figure 4.12). The results of the GE shown in Figure 4.13 confirmed 5' integration in all 4 clones.

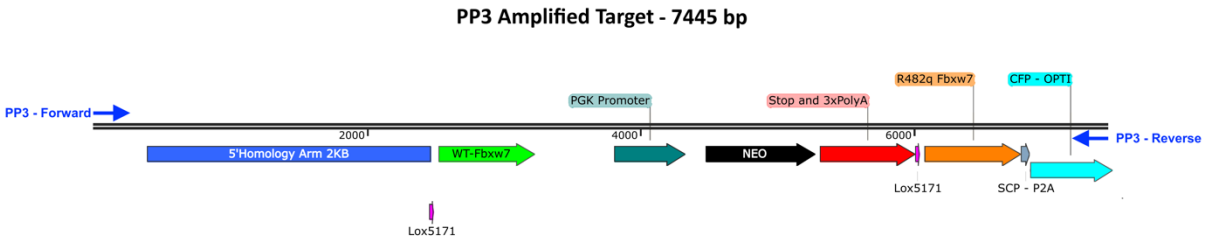

Figure 4.12. PCR product size in positive clones with 5' construct integration using primer pair 3 (PP3). Positive clones will amplify a PCR product of 7445 bp and wild type clones will have no detectable PCR product.

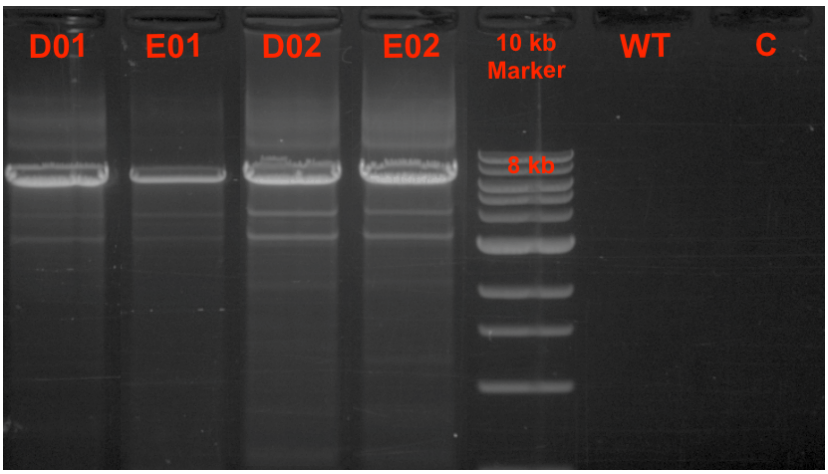

Figure 4.13 GE from PCR screening with primer pair 3 (PP3) to confirm 5' construct integration. Successful 5' integration produces a single band at 7445 bp. All 4 clones screened were confirmed for 5' construct integration. Wild type (WT) clones have no PCR product. C is a water control.

4.5 TAT-Cre treatment of confirmed embryonic stem cell clones

After confirming 5' and 3' construct integration, the Cre-dependent conditional KI was tested for functionality. All four positive mESC clones were treated with TAT-Cre recombinase to induce recombination between *loxP* sites. Successful Cre/*loxp* recombination will lead to a 3553 bp

deletion (Figure 4.12). TAT-Cre treated clones were viewed under epifluorescence microscopy with DAPI filter to visualise conditional expression of the CFP reporter gene. CFP is only expressed after Cre/*loxp* recombination and excision of the floxed STOP cassette. Images from the microscopy session can be seen in Figure 4.14. TAT-Cre treated clones had faintly increased fluorescence compared to non-treated clones.

As the images from the microscopy session were inclusive, TAT-Cre treated clones were lysed and DNA extracted for a PCR screening protocol. TAT-Cre treated cloned were screened were PCR amplified using PP3. Successful recombination between *loxP* site results in a 3553 bp deletion and consequently a PCR product of 3892 bp (Figure 4.12). The GE results shown in Figure 4.13 confirmed *loxP* recombination occurred in proportion of the cells in all four clones. Within the GE image strong bands are evident at both 7445 bp (no *loxP* recombination) and 3892 bp (*loxP* recombination).

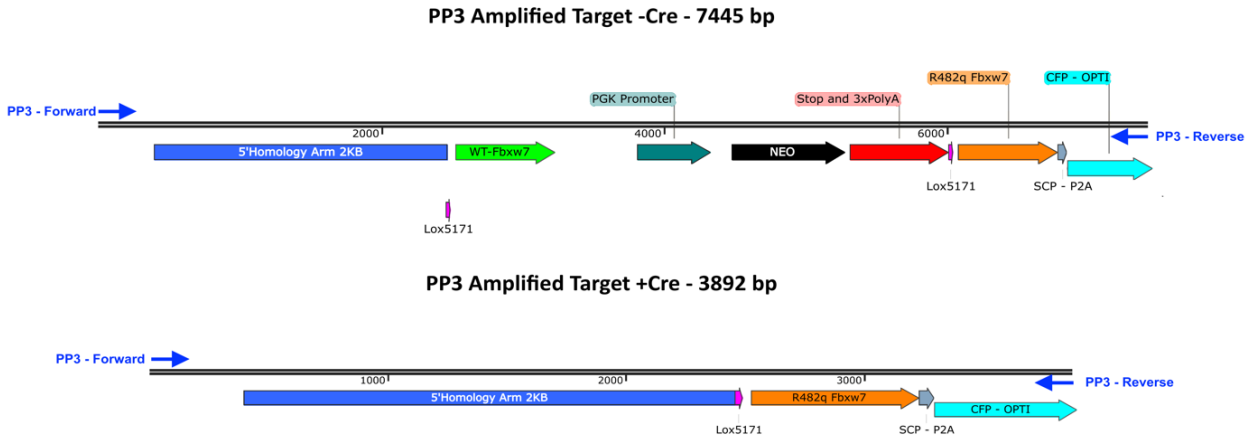

Figure 4.12 PCR product sizes in positive clones using primer pair 3 (PP3) both with (+Cre; 3892 bp) and without (-Cre; 7445 bp) TAT-Cre treatment. Wild type clones have no PCR product.

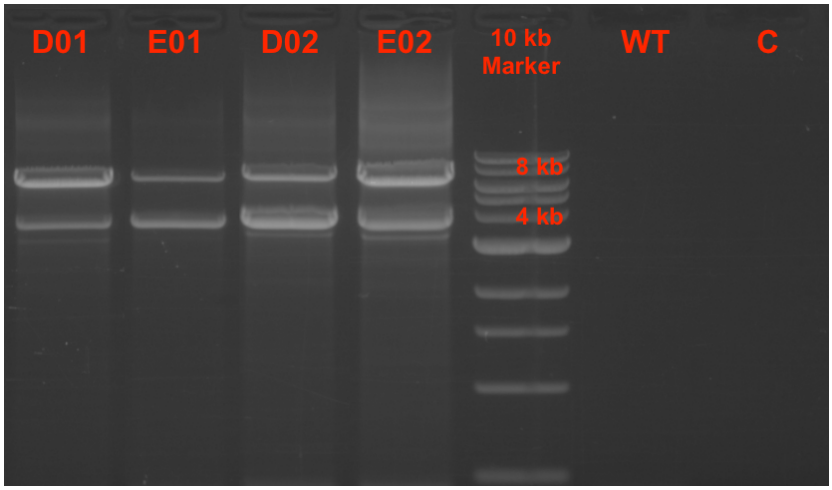

Figure 4.13 GE from PCR screening with primer pair 3 (PP3) of TAT-Cre treated mESC clones. Screen was to confirm Cre/*loxP* recombination events. All four clones treated with TAT-Cre generated a 3892 bp in a proportion of cells. This indicates recombination of the *loxP* sites was successful in a proportion of cells in all four clones. Wild type (WT) clones have no PCR product. C is a water control.

4.6 Blastocyst microinjection and offspring

Four positive mESC clones were confirmed at the completion of screening and functional testing. These clones were identified as D01, E01, D02 and E02. Each of these clones had stable and functional Cre-dependent conditional KI construct integration within intron 11 of the Fbxw7 gene. Frozen copies of two confirmed 'black coat' mESC clones (D01 and E01) were thawed and used for microinjection into 'white coat' Bl6-albion blastocysts. Injected blastocysts were transferred into CD1 foster mothers. The results of the microinjection session and the offspring are summarised in Table 4.2. Chimeric males from the litters were kept for further breeding. The percentage chimerism of the 10 males born was evaluated by visual assessment of the coat colour. Unfortunately, due to institutional policy at the WTCHG, no photography of experimental animals is permitted.

Table 4.2 Summary of the blastocyst microinjection session and the resulting litters.

mESC clone	Blastocysts injected	CD1 foster mothers	Mice born	Males born	Chimerism of males (%)
D01	36	2	5	4	95, 80, 80, 50
E01	38	2	11	6	95, 80, 80, 50, 0, 0

Figure 4.14 Epifluorescence microscopy of TAT-Cre treated clones. Each of the four positive clones (D01, D02, E01 and E02) was treat with (+Cre) and without (-Cre) TAT-Cre. Images were taken under phase contrast, and epifluorescence microscopy using a DAPI filter. All TAT-Cre treated clones have evidence of increased florescence due to CFP expression.

5 Discussion

This study sought to develop a cancer mouse model harbouring a 5.5 kb conditional KI within intron 11 of the Fbxw7 gene. The targeting construct used in this study contained a Cre-dependent conditional missense point mutation (R482Q) within exon 12 of Fbxw7. This point mutation is present in a diverse range of human cancers, including breast, lung and colorectal cancer (Babaei-Jadidi et al., 2011; Davis et al., 2011). A CRISPR/Cas9-meditated gene targeting strategy was used to generate mESCs for blastocyst microinjection. Direct gene targeting in mouse zygotes was not feasible due to the size and complexity of the Fbxw7 donor plasmid required to generate this large-scale conditional KI (17631 bp; Figure 2.2). Direct microinjection of donor plasmids into mouse zygotes have very low rates of integration, typically, 10 to 30% of zygotes carry the desired construct (Yang, Wang, & Jaenisch, 2014). As a CRISPR/Cas9-meditated gene targeting approach was employed, a gRNA targeting intron 11 in Fbxw7 was designed (Figure 4.1). On examination of the Fbxw7 target site it was evident that there were limited gRNA options that would not cleave of the Fbxw7 donor plasmid, whilst meeting the PAM requirements of SpCas9 and having an adequate predicted cutting efficiency. After systematic consideration, a gRNA was selected with a predicted cutting efficiency of 51 out of 100 at the Fbxw7 locus. This was calculated using the method developed by Fusi et al. (2015) and warranted further investigation to ensure sufficient cutting efficiency of the selected gRNA.

To experimentally investigate the cutting efficiency of the selected gRNA it was the tested in mouse melanoma cells. gRNA primers were subcloned into a CRISPR expression plasmid and the cloned plasmid was validated by restriction digestion before being confirmed by sequencing (Figure 4.2, 4.3 and 4.4). Melanocytes were then separately lipofected with the cCRISPR expression plasmid and a GFP expression plasmid. GFP expression in transfected cells confirmed an effective transfection protocol (Figure 4.5). Mouse melanoma cells successfully lipofected with the cCRISPR expression plasmid will express the unique gRNA and SpCas9, which, once complexed are capable of generating DSBs at the Fbxw7 target site in intron 11 (Figure 5.1). As no repair template was provided, CRISPR/Cas9-mediated DSBs are favourable repaired by the error prone NHEJ pathway, which often leaves indel mutations. To assess the frequency of indel mutations and consequently the cutting efficiency of the gRNA, a TIDE analysis was undertaken

using the software package designed by Brinkman et al. (2014). To do this, DNA was extracted from pools of CRISPR targeted melanocytes and non-targeted control melanocytes. The two DNA samples were separately sequenced across the gRNA target site. The quantitative trace data from the two Sanger sequencing reaction was then used by the TIDE software to determine the total cutting efficiency of the gRNA to be 33.2% (Figure 4.6a). Previous gRNA efficiencies measured at the WTCHG indicated this was sufficient to progress to gene targeting in mESCs. The TIDE software also generated a quality assurance graph that indicated that aberrations >20% between the control and Fbxw7 targeted sequences originate proximal to the expected gRNA cut site (Within 12 bp; Figure 2.5b).

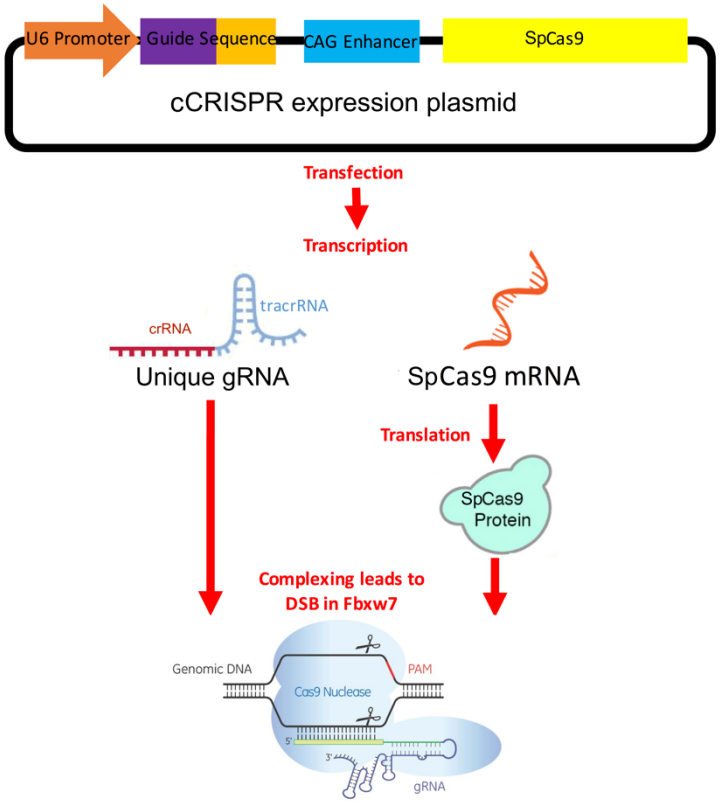

Figure 5.1 Cloned CRISPR (cCRISPR) expression plasmid. In mammalian cells this plasmid expresses the essential components for CRISPR/Cas9 gene targeting. The CRISPR expressed components are the unique gRNA and SpCas9 mRNA for translation into SpCas9 protein. Within this project, complexing of the gRNA and SpCas9 leads to cleavage at Fbxw7 target site in intron 11.

Although the gRNA efficiency was evaluated in the melanoma cells, the specificity of the gRNA was not examined *in vitro*. Perhaps the greatest concern regarding CRISPR/Cas9 is the issue of off target effects. A number of studies in mammalian cells have documented off target mutations

occurring at significant rates at sites with sequence similarity to the on target sites (Cho et al., 2014; Fu et al., 2013; Hsu et al., 2013). Off target effects could confound phenotypic analyses of the resulting *Fbxw7*^{R482Q} mouse model. It has been demonstrated that, although each nucleotide within the 20 nt crRNA segment of the gRNA contributes to overall SpCas9 specificity, single mismatches are often well tolerated, and several mismatches can also be tolerated depending on their location within crRNA sequence and the context within the genome (Hsu et al., 2013; Pattanayak et al., 2013). Experimental protocols for screening off target effects are laborious, costly and time consuming, and is not yet a routine procedure for CRISPR/Cas9 GM mouse production. Instead an *in silico* based approach for determining off target potential of the gRNA was employed in this study. Within the mouse genome (GRCm38/mm10) the designed 20 nt crRNA portion of the gRNA had no additional target sites with 0 or 1 nt mismatches. However, for crRNA mismatches of 2, 3 and 4 nt there were 1, 15 and 125 off-target sites, respectively (Table 4.1). These computational results suggested the gRNA had minimal potential for off target effects in the mouse genome.

The optimisation and validation gRNA design is critical for reducing off target potential, however, alternative methods to improve the specificity of CRISPR/Cas9 have been developed. One strategy is to use different Cas9 systems, such as *N. meningitides,* which can offer better targeting specificity by virtue of its longer crRNA (24 nt for *N. meningitidis*) and longer PAM sequence (5'-NNNNGATT for *N. meningitides;* Hou et al., 2013). Another strategy has been to use a modified version of SpCas9 that can only introduce a single-strand nick at the target site, rather than a DSB. Use of a pair of 'nickase' Cas9 complexes with binding sites on opposite strands of the target sequence can produce the equivalent of a DSB with 5' overhangs. At an off-target site, a single-strand nick would be repaired by a different mechanism, known as the base excision repair pathway, which is much less likely to leave indel mutations. Since the likelihood of two nickases binding nearby each other elsewhere in the genome is very low, the off target mutation rate is greatly reduced. Indeed, testing of this nickase systems in mammalian cells has demonstrated up to a threefold reduction in off target activity with only a slight reduction in on target efficacy (Cho et al., 2014; Ran et al.).

After verifying the efficiency and specificity of the selected gRNA, the study was progressed to gene targeting in mESCs. For this, the cCRISPR expression plasmid and Fbxw7 donor plasmid were electroporated in mESCs. The simultaneous transfection of the cCRISPR expression plasmid and the Fbxw7 donor plasmid was aimed at inducing mESCs to repair the CRISPR/Cas9-mediated DSB via HDR and thus copy the targeting construct into the break site. Figure 5.2 shows a schematic diagram of CRISPR/Cas9-mediated HDR using the Fbxw7 donor plasmid as a template. As the transfected cCRISPR expression plasmid contained a puromycin resistance gene, and the Fbxw7 donor plasmid was designed with a neomycin resistance gene and diphtheria toxin A cassette located outside the homology arms, this allowed for both positive and negative selection in transfected mESCs. After eight days of selection, 22 mESC clones were picked and expanded. Of the 22 clones, 4 were confirmed for 5' and 3' construct integration by series of three PCR screening protocols. However, PCR screening approaches cannot detect concurrent random integration and, therefore, full characterization requires Southern blotting (Wang et al., 2015). Although highly recommended, Southern blotting was not performed in this study. This decision was made with the foresight that 2 of the 4 clones will be used for blastocyst microinjection and all established mice lines undergo a complete characterization.

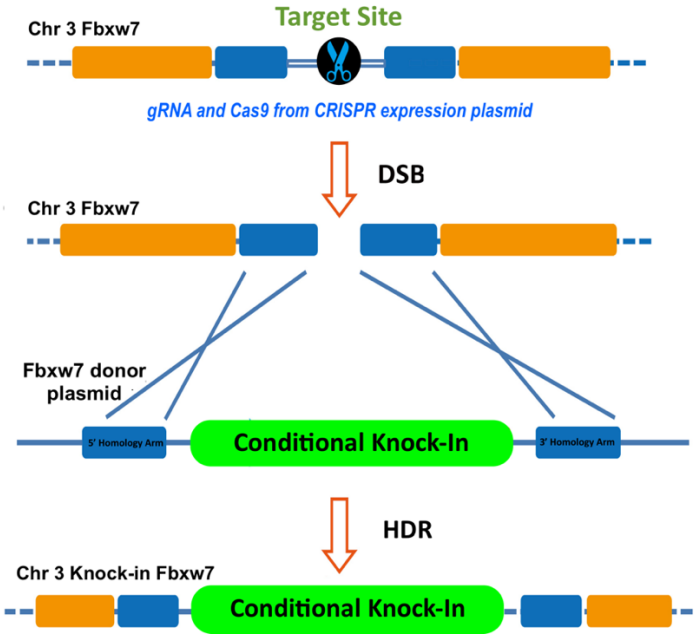

Figure 5.2 CRISPR/Cas9-medaited gene targeting with Fbxw7 donor plasmid. SpCas9 and gRNA are expressed from the cCRISPR expression plasmid. A complex between gRNA and SpCas9 is formed which generates a DSB at the target site. The Fbxw7 donor plasmid then induces the cell to repair the DSB via HDR and thus copy's the 5.5 kb conditional knock-in construct into the cut site.

The targeting construct used in this study took advantage of a Cre-dependent conditional KI system. Once integrated, this construct design will ultimately allow investigators to study the Fbxw7(R482Q) point mutation in specific cell lineage or at a specific developmental stage. The conditional KI system used in the Fbxw7 donor plasmid is known as the 'minigene' method (Figure 1.6b). The minigene method in the conditional KI construct contains a WT Fbxw7 minigene (an intronless gene segment that contains exon 12, 13 and 14) and a STOP cassette, which are collectively floxed. Directly downstream from the floxed minigene system is the mutant Fbxw7(R482Q) allele and a CFP reporter gene. In the presence of Cre recombinase, recombination between the *loxP* sites will occur, resulting in excision of the floxed 3.5kb DNA sequence containing the WT Fbxw7 minigene and STOP cassette (Figure 5.3). Following recombination of the *loxP* sites, the mutant Fbxw7(R482Q) allele and a CFP report gene will be expressed from their natural promoter. By including the CFP reporter gene in the construct it allows scientists to visually identify cells that are expressing the conditional mutant Fbxw7(R482Q) allele.

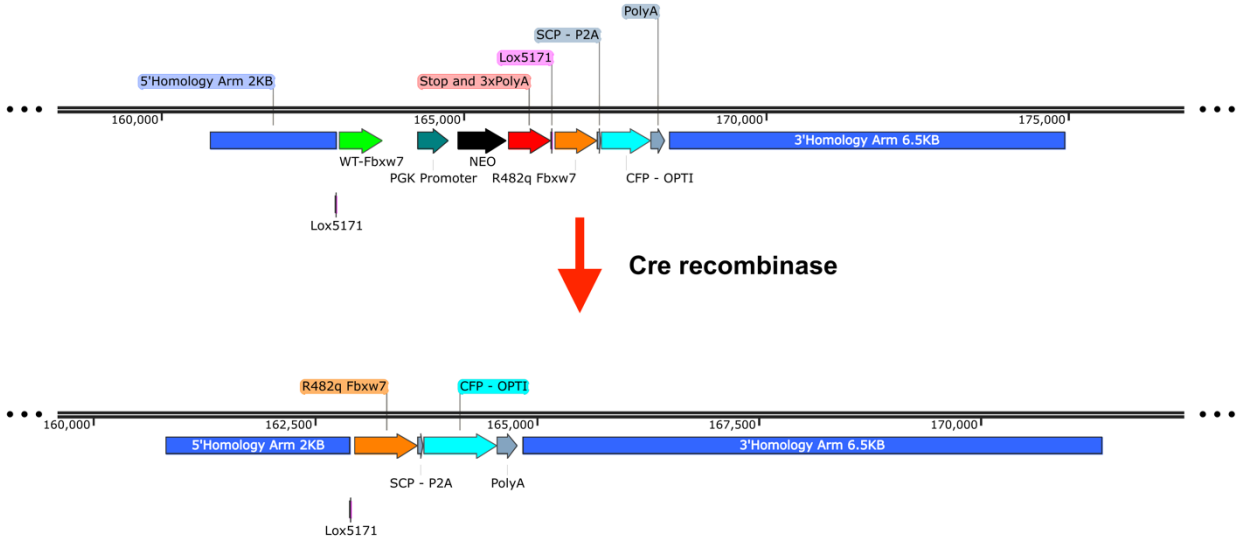

Figure 5.3 Fbxw7 conditional knock-in construct, with and without Cre recombination. Recombination of the *loxP* sites results in 3553 bp deletion, which includes the WT Fbxw7 minigene and STOP cassette that prevent expression of the mutant Fbxw7(R482Q) and CFP reporter gene.

To test the functionality of the conditional KI system in the four positive mESC clones, TAT-Cre recombinase was added to cells at 40% confluent. Once confluent, TAT-Cre treated clones were viewed under an epifluorescence microscope using a DAPI filter to visualise CFP expression. The images obtained from the microscopy session showed faint evidence of increased fluorescence

from CFP expression in TAT-Cre treated cells (Figure 4.14). To improve these findings, optimization of the TAT-Cre treatment protocol may increase CFP expression. Additionally, the use of a confocal fluorescence microscope as opposed to a standard epifluorescence microscope may allow for easier detection of CFP. As the microscopy session offered inclusive results, the functionality of the conditional KI system in the TAT-Cre treated clones required further investigation. To do this TAT-Cre clones were lysed and DNA extracted. Using a PCR based approach it was confirmed that the predicted 3.5 kb DNA sequence had been deleted from a proportion of cells in all four TAT-Cre treated clones (Figure 4.13). This indicated that Cre-mediated recombination between the *loxP* sites had occurred. These findings confirmed that the Cre-dependent conditional KI system was functional in all four confirmed mESC clones.

Following successful screening and functional testing, two of the four confirmed mESC clones (D01 and E01) were thawed from frozen copies and prepared for blastocyst microinjection. The positive mESCs were developed on a male 'black coat' JM8.F6 mESC background and injected into 'white coat' Bl6-albino blastocysts before being transferred into CD1 fosters mothers. Male mESCs were used to favour the development of male offspring, which are beneficial for future breeding. Successful integration of mESCs into the inner cell mass of the blastocysts results in black and white chimeric pups. The desired outcome was to generate germline competent chimeric males for germline transmission. Four litters were produced with a total of 8 chimeric males born that ranged in chimerism from 50 to 95% (Table 4.2). The percentage black coat colour was used to estimate the contribution of the mESC to the mice. However, it should be noted that coat colour does not fully reflect the injected mESCs contribution to the germ cells (Carstea et al., 2009). Currently, two 95% chimeric males are set for mating with white albino females in the hope of generating heterozygous *Fbxw7*^{R482Q} (F1) offspring (Figure 5.4). Germline transmission of the mESC derived genes will result in black pups due to dominant inheritance of the black coat colour. Once a breeding population is established the Tomlinson group at the WTCHG plans to cross the *Fbxw7*^{R482Q} mice with *Villin-Cre* mice. *Villin-Cre* mice express Cre recombinase in villus and crypt epithelial cells of the small and large intestines. Crossing of the *Fbxw7*^{R482Q} mice with the *VIllin-Cre* mice will allow the Tomlinson group to study the role of the Fbxw7(R482Q) missense point mutation in the development of colorectal cancer.

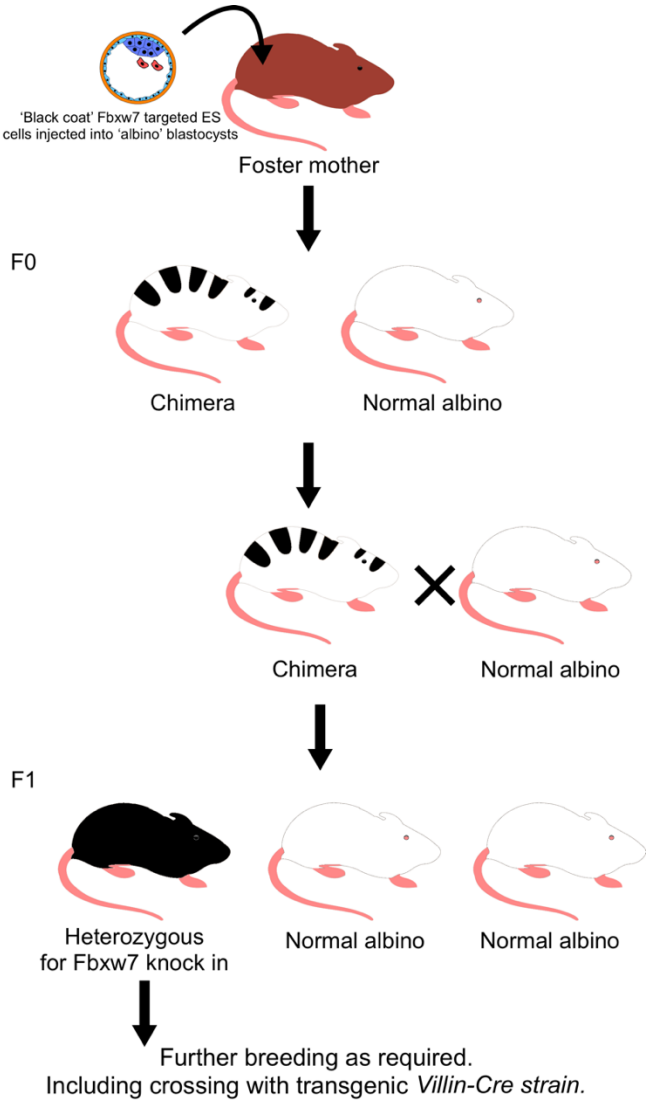

Figure 5.4 Breeding scheme to generate heterozygous *Fbxw7*^{R482Q} (F1) from chimeric males (F0). Future plans are to cross *Fbxw7*^{R482Q} mice with *Villin-Cre* mice to study the role of the Fbxw7(R482Q) mutation in the development of colorectal cancer. Image was modified and adapted from Lodish et al. (2000).

6 Conclusion

In summary, the application of CRISPR/Cas9 in mESCs remains the 'gold standard' for generating large-scale conditional KI mouse models. This study successfully employed a CRISPR/Cas9-mediated gene targeting approach in mESCs to generate conditional KI chimeric male mice to be used for germline transmission. To limit off target effects and enhance productivity, the CRISPR gRNA used in this study was tested via combination of *in vitro* and *in silico* based methods to validate both efficiency and specificity. The construct integrated into CRISPR/Cas9 target site in intron 11 of the Fbxw7 gene was a 5.5 kb Cre-dependent conditional KI that harboured a missense point mutation (Fbxw7(R482Q)) in exon 12. Fbxw7(R482Q) is found in a diverse range of human cancers. The targeting construct also included a CFP reporter gene to track expression of the mutant Fbxw7 allele. Following PCR based screening and functional testing of the targeted mESCs, two confirmed clones were microinjected into WT blastocysts. From the resulting four litters, eight chimeric males were born with up to 95% chimerism based on coat colour. Two 95% chimeric males are currently set for mating WT females in the hope of gaining germline transmission of the mESC derived genes. Successful transmission will generate heterozygous *Fbxw7*^{R482Q} mice. The Tomlinson group at the WTCHG plans to cross the *Fbxw7*^{R482Q} mouse model with *Villin-Cre* transgenic mice. This will enable the group to study the role Fbxw7(R482Q) point mutation in development of colorectal cancer.

References

Babaei-Jadidi, R., Li, N., Saadeddin, A., Spencer-Dene, B., Jandke, A., Muhammad, B., . . . Nateri, A. S. (2011). FBXW7 influences murine intestinal homeostasis and cancer, targeting Notch, Jun, and DEK for degradation. *J Exp Med, 208*(2), 295-312. doi:10.1084/jem.20100830

Bayascas, J. R., Sakamoto, K., Armit, L., Arthur, J. S., & Alessi, D. R. (2006). Evaluation of approaches to generation of tissue-specific knock-in mice. *J Biol Chem, 281*(39), 28772-28781. doi:10.1074/jbc.M606789200

Behringer, R., Gertsenstein, M., Nagy, K. V., & Nagy, A. (2014). *Manipulating the Mouse Embryo: A Laboratory Manual* (4th ed.). New York: CSH Laboratory Press.

Bolukbasi, M. F., Gupta, A., Oikemus, S., Derr, A. G., Garber, M., Brodsky, M. H., . . . Wolfe, S. A. (2015). DNA-binding-domain fusions enhance the targeting range and precision of Cas9. *Nat Methods, 12*(12), 1150-1156. doi:10.1038/nmeth.3624

Brinkman, E. K., Chen, T., Amendola, M., & van Steensel, B. (2014). Easy quantitative assessment of genome editing by sequence trace decomposition. *Nucleic Acids Research, 42*(22), e168-e168.

Capecchi, M. R. (1989). Altering the genome by homologous recombination. *Science, 244*(4910), 1288-1292.

Capecchi, M. R. (1994). Targeted gene replacement. *Scientific American*(270), 34.

Carstea, A. C., Pirity, M. K., & Dinnyes, A. (2009). Germline competence of mouse ES and iPS cell lines: Chimera technologies and genetic background. *World Journal of Stem Cells, 1*(1), 22-29. doi:10.4252/wjsc.v1.i1.22

Chandrasegaran, S., & Carroll, D. (2016). Origins of Programmable Nucleases for Genome Engineering. *J Mol Biol, 428*(5 Pt B), 963-989. doi:10.1016/j.jmb.2015.10.014

Chen, S., Lee, B., Lee, A. Y., Modzelewski, A. J., & He, L. (2016). Highly Efficient Mouse Genome Editing by CRISPR Ribonucleoprotein Electroporation of Zygotes. *J Biol Chem, 291*(28), 14457-14467. doi:10.1074/jbc.M116.733154

Cho, S. W., Kim, S., Kim, Y., Kweon, J., Kim, H. S., Bae, S., & Kim, J.-S. (2014). Analysis of off-target effects of CRISPR/Cas-derived RNA-guided endonucleases and nickases. *Genome Research, 24*(1), 132-141. doi:10.1101/gr.162339.113

Cong, L., Ran, F. A., Cox, D., Lin, S., Barretto, R., Habib, N., . . . Zhang, F. (2013). Multiplex genome engineering using CRISPR/Cas systems. *Science, 339*(6121), 819-823. doi:10.1126/science.1231143

Davis, H., Lewis, A., Behrens, A., & Tomlinson, I. (2014). Investigation of the atypical FBXW7 mutation spectrum in human tumours by conditional expression of a heterozygous propellor tip missense allele in the mouse intestines. *Gut, 63*(5), 792-799. doi:10.1136/gutjnl-2013-304719

Davis, H., Lewis, A., Spencer-Dene, B., Tateossian, H., Stamp, G., Behrens, A., & Tomlinson, I. (2011). FBXW7 mutations typically found in human cancers are distinct from null alleles and disrupt lung development. *J Pathol, 224*(2), 180-189. doi:10.1002/path.2874

Doyle, A., McGarry, M. P., Lee, N. A., & Lee, J. J. (2012). The Construction of Transgenic and Gene Knockout/Knockin Mouse Models of Human Disease. *Transgenic research, 21*(2), 327-349. doi:10.1007/s11248-011-9537-3

Folger, K., Thomas, K., & Capecchi, M. R. (1984). Analysis of homologous recombination in cultured mammalian cells. *Cold Spring Harb Symp Quant Biol*(49), 123.

Fu, Y., Foden, J. A., Khayter, C., Maeder, M. L., Reyon, D., Joung, J. K., & Sander, J. D. (2013). High-frequency off-target mutagenesis induced by CRISPR-Cas nucleases in human cells. *Nat Biotechnol, 31*(9), 822-826. doi:10.1038/nbt.2623

Fujii, W., Kawasaki, K., Sugiura, K., & Naito, K. (2013). Efficient generation of large-scale genome-modified mice using gRNA and CAS9 endonuclease. *Nucleic Acids Res, 41*(20), e187. doi:10.1093/nar/gkt772

Fusi, N., Smith, I., Doench, J., & Listgarten, J. (2015). In Silico Predictive Modeling of CRISPR/Cas9 guide efficiency. *bioRxiv*.

Gaj, T., Gersbach, C. A., & Barbas, C. F., 3rd. (2013). ZFN, TALEN, and CRISPR/Cas-based methods for genome engineering. *Trends Biotechnol, 31*(7), 397-405. doi:10.1016/j.tibtech.2013.04.004

Gordon, J. W., Scangos, G. A., Plotkin, D. J., Barbosa, J. A., & Ruddle, F. H. (1980). Genetic transformation of mouse embryos by microinjection of purified DNA. *Proceedings of the National Academy of Sciences, 77*(12), 7380-7384.

Gupta, R. M., & Musunuru, K. (2014). Expanding the genetic editing tool kit: ZFNs, TALENs, and CRISPR-Cas9. *J Clin Invest, 124*(10), 4154-4161. doi:10.1172/JCI72992

Haeussler, M., Schönig, K., Eckert, H., Eschstruth, A., Mianné, J., Renaud, J.-B., . . . Concordet, J.-P. (2016). Evaluation of off-target and on-target scoring algorithms and integration into the guide RNA selection tool CRISPOR. *Genome Biology, 17*(1), 1-12. doi:10.1186/s13059-016-1012-2

Hall, B., Limaye, A., & Kulkarni, A. B. (2009). Overview: Generation of Gene Knockout Mice. *Current protocols in cell biology / editorial board, Juan S. Bonifacino ... [et al.], CHAPTER*, Unit-19.1217. doi:10.1002/0471143030.cb1912s44

Horvath, P., & Barrangou, R. (2010). CRISPR/Cas, the immune system of bacteria and archaea. *Science, 327*(5962), 167-170. doi:10.1126/science.1179555

Hou, Z., Zhang, Y., Propson, N. E., Howden, S. E., Chu, L.-F., Sontheimer, E. J., & Thomson, J. A. (2013). Efficient genome engineering in human pluripotent stem cells using Cas9 from Neisseria meningitidis. *Proc Natl Acad Sci U S A, 110*(39), 15644-15649. doi:10.1073/pnas.1313587110

Hsu, P. D., Scott, D. A., Weinstein, J. A., Ran, F. A., Konermann, S., Agarwala, V., . . . Zhang, F. (2013). DNA targeting specificity of RNA-guided Cas9 nucleases. *Nat Biotech, 31*(9), 827-832. doi:10.1038/nbt.2647

http://www.nature.com/nbt/journal/v31/n9/abs/nbt.2647.html - supplementary-information

Hughes, E. D., & Saunders, T. L. (2011). Gene Targeting in Embryonic Stem Cells. 291-325. doi:10.1007/978-3-662-45763-4_14

Ishino, Y., Shinagawa, H., Makino, K., Amemura, M., & Nakata, A. (1987). Nucleotide sequence of the iap gene, responsible for alkaline phosphatase isozyme conversion in Escherichia coli, and identification of the gene product. *Journal of Bacteriology, 169*(12), 5429-5433.

Ittner, L., & Delerue, F. (2015). Genome Editing in Mice Using CRISPR/Cas9: Achievements and Prospects. *Cloning & Transgenesis, 04*(01). doi:10.4172/2168-9849.1000135

Jinek, M., Chylinski, K., Fonfara, I., Hauer, M., Doudna, J. A., & Charpentier, E. (2012). A Programmable Dual-RNA–Guided DNA Endonuclease in Adaptive Bacterial Immunity. *Science, 337*(6096), 816-821.

Kim, H., & Kim, J. S. (2014). A guide to genome engineering with programmable nucleases. *Nat Rev Genet, 15*(5), 321-334. doi:10.1038/nrg3686

Kwan, K. M. (2002). Conditional alleles in mice: practical considerations for tissue-specific knockouts. *Genesis, 32*(2), 49-62.

Lodish, H., Berk, A., Zipursky, A. L., Matsudaira, P., Baltimore, D., & Darnell, J. (2000). *Molecular Cell Biology* (4th ed.). New York, New York: Palgrave Macmillan.

Martin, G. R. (1981). Isolation of a pluripotent cell line from early mouse embryos cultured in medium conditioned by teratocarcinoma stem cells. *Proc Natl Acad Sci U S A, 78*(12), 7634-7638.

Meyers, E. N., Lewandoski, M., & Martin, G. R. (1998). An Fgf8 mutant allelic series generated by Cre- and Flp-mediated recombination. *Nat Genet, 18*(2), 136-141. doi:10.1038/ng0298-136

Mojica, F. J., & Montoliu, L. (2016). On the Origin of CRISPR-Cas Technology: From Prokaryotes to Mammals. *Trends Microbiol*. doi:10.1016/j.tim.2016.06.005

Moore, J. D. (2015). The impact of CRISPR-Cas9 on target identification and validation. *Drug Discov Today, 20*(4), 450-457. doi:10.1016/j.drudis.2014.12.016

Müller, U. (1999). Ten years of gene targeting: targeted mouse mutants, from vector design to phenotype analysis. *Mechanisms of Development, 82*(1–2), 3-21. doi:http://dx.doi.org/10.1016/S0925-4773(99)00021-0

Nakayama, K. I., & Nakayama, K. (2006). Ubiquitin ligases: cell-cycle control and cancer. *Nat Rev Cancer, 6*(5), 369-381. doi:10.1038/nrc1881

Palmiter, R. D., Brinster, R. L., Hammer, R. E., Trumbauer, M. E., Rosenfeld, M. G., Birnberg, N. C., & Evans, R. M. (1982). Dramatic growth of mice that develop from eggs microinjected with metallothionein-growth hormone fusion genes. *Nature, 300*(5893), 611-615.

Pattanayak, V., Lin, S., Guilinger, J. P., Ma, E., Doudna, J. A., & Liu, D. R. (2013). High-throughput profiling of off-target DNA cleavage reveals RNA-programmed Cas9 nuclease specificity. *Nat Biotech, 31*(9), 839-843. doi:10.1038/nbt.2673

http://www.nature.com/nbt/journal/v31/n9/abs/nbt.2673.html - supplementary-information

Peters, L. L., Robledo, R. F., Bult, C. J., Churchill, G. A., Paigen, B. J., & Svenson, K. L. (2007). The mouse as a model for human biology: a resource guide for complex trait analysis. *Nat Rev Genet, 8*(1), 58-69.

Ran, F. A., Hsu, Patrick D., Lin, C.-Y., Gootenberg, Jonathan S., Konermann, S., Trevino, A. E., . . . Zhang, F. Double Nicking by RNA-Guided CRISPR Cas9 for Enhanced Genome Editing Specificity. *Cell, 154*(6), 1380-1389. doi:10.1016/j.cell.2013.08.021

Rappaport, A., & Johnson, L. (2014). Genetically engineered knock-in and conditional knock-in mouse models of cancer. *Cold Spring Harb Protoc, 2014*(9), 897-911. doi:10.1101/pdb.top069799

Rocha-Martins, M., Cavalheiro, G. R., Matos-Rodrigues, G. E., & Martins, R. A. (2015). From Gene Targeting to Genome Editing: Transgenic animals applications and beyond. *An Acad Bras Cienc, 87*(2 Suppl), 1323-1348. doi:10.1590/0001-3765201520140710

Rouet, P., Smih, F., & Jasin, M. (1994). Introduction of double-strand breaks into the genome of mouse cells by expression of a rare-cutting endonuclease. *Molecular and Cellular Biology, 14*(12), 8096-8106.

Sander, J. D., & Joung, J. K. (2014). CRISPR-Cas systems for editing, regulating and targeting genomes. *Nat Biotechnol, 32*(4), 347-355. doi:10.1038/nbt.2842

Sato, M., Ohtsuka, M., Watanabe, S., & Gurumurthy, C. B. (2016). Nucleic acids delivery methods for genome editing in zygotes and embryos: the old, the new, and the old-new. *Biol Direct, 11*(1), 16. doi:10.1186/s13062-016-0115-8

Seruggia, D., & Montoliu, L. (2014). The new CRISPR-Cas system: RNA-guided genome engineering to efficiently produce any desired genetic alteration in animals. *Transgenic Res, 23*(5), 707-716. doi:10.1007/s11248-014-9823-y

Shen, B., Zhang, W., Zhang, J., Zhou, J., Wang, J., Chen, L., . . . Skarnes, W. C. (2014). Efficient genome modification by CRISPR-Cas9 nickase with minimal off-target effects. *Nat Methods, 11*(4), 399-402. doi:10.1038/nmeth.2857

Singh, P., Schimenti, J. C., & Bolcun-Filas, E. (2015). A mouse geneticist's practical guide to CRISPR applications. *Genetics, 199*(1), 1-15. doi:10.1534/genetics.114.169771

Skarnes, W. C. (2015). Is mouse embryonic stem cell technology obsolete? *Genome Biol, 16*, 109. doi:10.1186/s13059-015-0673-6

Smih, F., Rouet, P., Romanienko, P. J., & Jasin, M. (1995). Double-strand breaks at the target locus stimulate gene targeting in embryonic stem cells. *Nucleic Acids Research, 23*(24), 5012-5019.

Smithies, O., Gregg, R. G., Boggs, S. S., Koralewski, M. A., & Kucherlapati, R. S. (1985). Insertion of DNA sequences into the human chromosomal beta-globin locus by homologous recombination. *Nature, 317*(6034), 230-234.

Tahimic, C. G. T., Sakurai, K., Aiba, K., & Nakatsuji, N. (2013). Cre/loxP, Flp/FRT Systems and Pluripotent Stem Cell Lines. In S. Renault & P. Duchateau (Eds.), *Site-directed insertion of transgenes* (pp. 189-209). Dordrecht: Springer Netherlands.

Tsai, S. Q., Wyvekens, N., Khayter, C., Foden, J. A., Thapar, V., Reyon, D., . . . Joung, J. K. (2014). Dimeric CRISPR RNA-guided FokI nucleases for highly specific genome editing. *Nat Biotech, 32*(6), 569-576. doi:10.1038/nbt.2908

http://www.nature.com/nbt/journal/v32/n6/abs/nbt.2908.html - supplementary-information

Urnov, F. D., Rebar, E. J., Holmes, M. C., Zhang, H. S., & Gregory, P. D. (2010). Genome editing with engineered zinc finger nucleases. *Nat Rev Genet, 11*(9), 636-646. doi:10.1038/nrg2842

Vandamme, T. F. (2015). Rodent models for human diseases. *European Journal of Pharmacology, 759*, 84-89. doi:http://dx.doi.org/10.1016/j.ejphar.2015.03.046

Wang, B., Li, K., Wang, A., Reiser, M., Saunders, T., Lockey, R. F., & Wang, J. W. (2015). Highly efficient CRISPR/HDR-mediated knock-in for mouse embryonic stem cells and zygotes. *Biotechniques, 59*(4), 201-202, 204, 206-208. doi:10.2144/000114339

Williams, A., Henao-Mejia, J., & Flavell, R. A. (2016). Editing the Mouse Genome Using the CRISPR-Cas9 System. *Cold Spring Harb Protoc, 2016*(2), pdb top087536. doi:10.1101/pdb.top087536

Yang, H., Wang, H., & Jaenisch, R. (2014). Generating genetically modified mice using CRISPR/Cas-mediated genome engineering. *Nat. Protocols, 9*(8), 1956-1968. doi:10.1038/nprot.2014.134

http://www.nature.com/nprot/journal/v9/n8/abs/nprot.2014.134.html - supplementary-information

Yang, H., Wang, H., Shivalila, Chikdu S., Cheng, Albert W., Shi, L., & Jaenisch, R. (2014). One-Step Generation of Mice Carrying Reporter and Conditional Alleles by CRISPR/Cas-Mediated Genome Engineering. *Cell, 154*(6), 1370-1379. doi:10.1016/j.cell.2013.08.022

Yoshimi, K., Kunihiro, Y., Kaneko, T., Nagahora, H., Voigt, B., & Mashimo, T. (2016). ssODN-mediated knock-in with CRISPR-Cas for large genomic regions in zygotes. *Nat Commun, 7*, 10431. doi:10.1038/ncomms10431

Appendices

Appendix A – Function of plasmid features

Table A.1 Function of CRISPR expression plasmid features

Plasmid features	Function
E. coli Replication Origin	Origin for plasmid replication in E. coli during amplification.
U6 Promoter	Drives expression of gRNA and SpCas9 in mammalian cells.
BbsI	Restriction sites used to clone gRNA primers into plasmid.
CAG Enhancer	Enhances expression of SpCas9.
Cas9	Encodes for *Streptococcus pyogenes* CRISPR associated protein 9 (SpCas9), which is a RNA-guided DNA endonuclease.
BGH Poly Terminator	Bovine growth hormone polyadenylation, which is a mammalian transcription termination sequence.
PGK Promoter and Puro Resistance	Phosphoglycerate kinase promoter that drives expression of puromycin resistance gene in mammalian cells.
Ampicillin Resistance	Confers ampicillin resistance to E. coli during plasmid amplification.

Table A.2 Function of Fbxw7 donor plasmid features

Plasmid feature	Function
E. Coli Replication Origin	Origin for plasmid replication in E. coli during amplification.
Ampicillin Resistance	Confers ampicillin resistance to E. coli during plasmid amplification.
5’ Homology Arm 2KB	5’ homology arm to induce HDR after DSB by SpCas9.
Lox5171	The active sites for Cre recombinase, which recombines the pair of *loxP* sites in the construct.
WT-Fbxw7	Wild type version of Fbxw7.
PGK Promoter	Phosphoglycerate kinase promoter to drive expression of neomycin resistance in mammalian cells.
NEO	Confers neomycin resistance in mammalian cells. This cassette is used for positive selection.
Stop and 3xPolyA	Terminates further expression of the construct in mammalian cells.
R482q – Fbxw7	Mutant version of Fbxw7 that contains the R482Q missense point mutation in exon 12.
SCP – P2A	Splits a single transcript into two for translation into two proteins.
CFP – OPTI	Optimised cyan fluorescent protein for detection of R482q – Fbxw7 expression.
PolyA	Terminates transcription.
3’ Homology Arm 6.5KB	3’ homology arm to induce HDR after DSB by SpCas9.
Diphtheria Toxin A	Encodes for diphtheria toxin A. This toxin is used as a negative selection cassette, preventing random integration into the genome by causing cell death

Table A.3 Function of GFP expression plasmid features

Plasmid features	Function
CAG Promoter	Strong synthetic promoter used to drive high levels of expression of eGFP in mammalian cells.
eGFP	Encodes for enhanced green fluorescent protein (GFP)
Rabbit beta globin poly-A	Terminates transcription.
Origin of Replication (pUC)	Origin for plasmid replication in E. coli during amplification.
Ampicillin Resistance	Confers ampicillin resistance to E. coli during plasmid amplification.

Appendix B – Spectrophotometry results of plasmid purifications

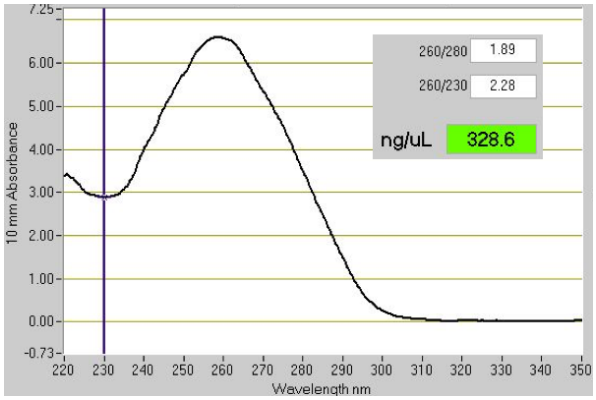

Figure B.1 NanoDrop™ spectrophotometry results for CRISPR expression plasmid purification.

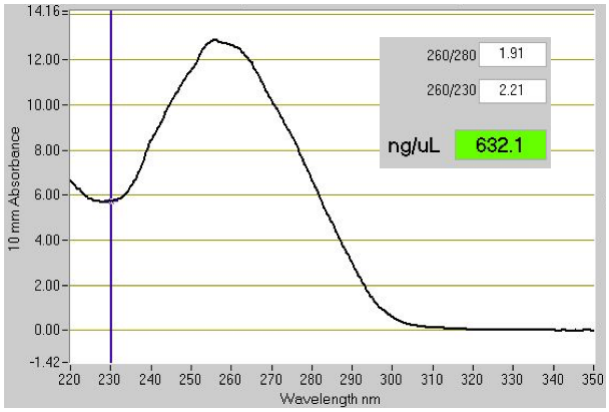

Figure B.2 NanoDrop™ spectrophotometry results for Fbxw7 donor plasmid purification.

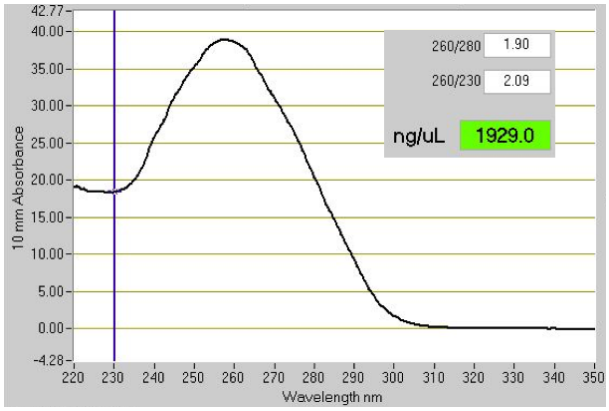

Figure B.3 NanoDrop™ spectrophotometry results for GFP expression plasmid purification.

Appendix C – Timeline scheme of cell culture procedures

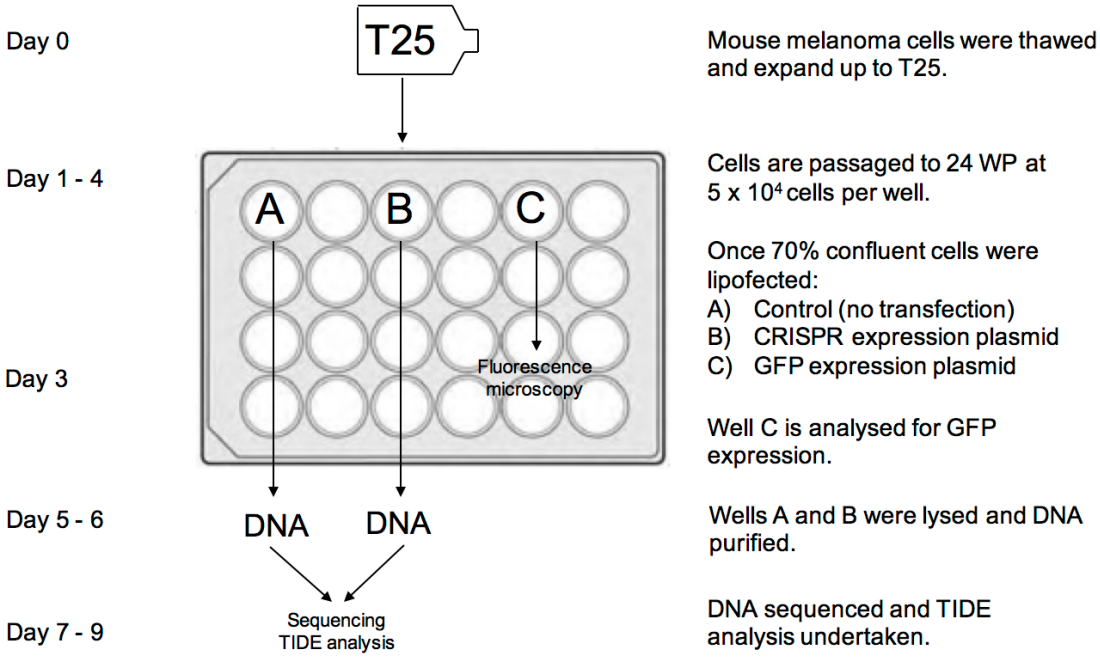

Figure C.1 Melanoma cell culture procedures and timeline.

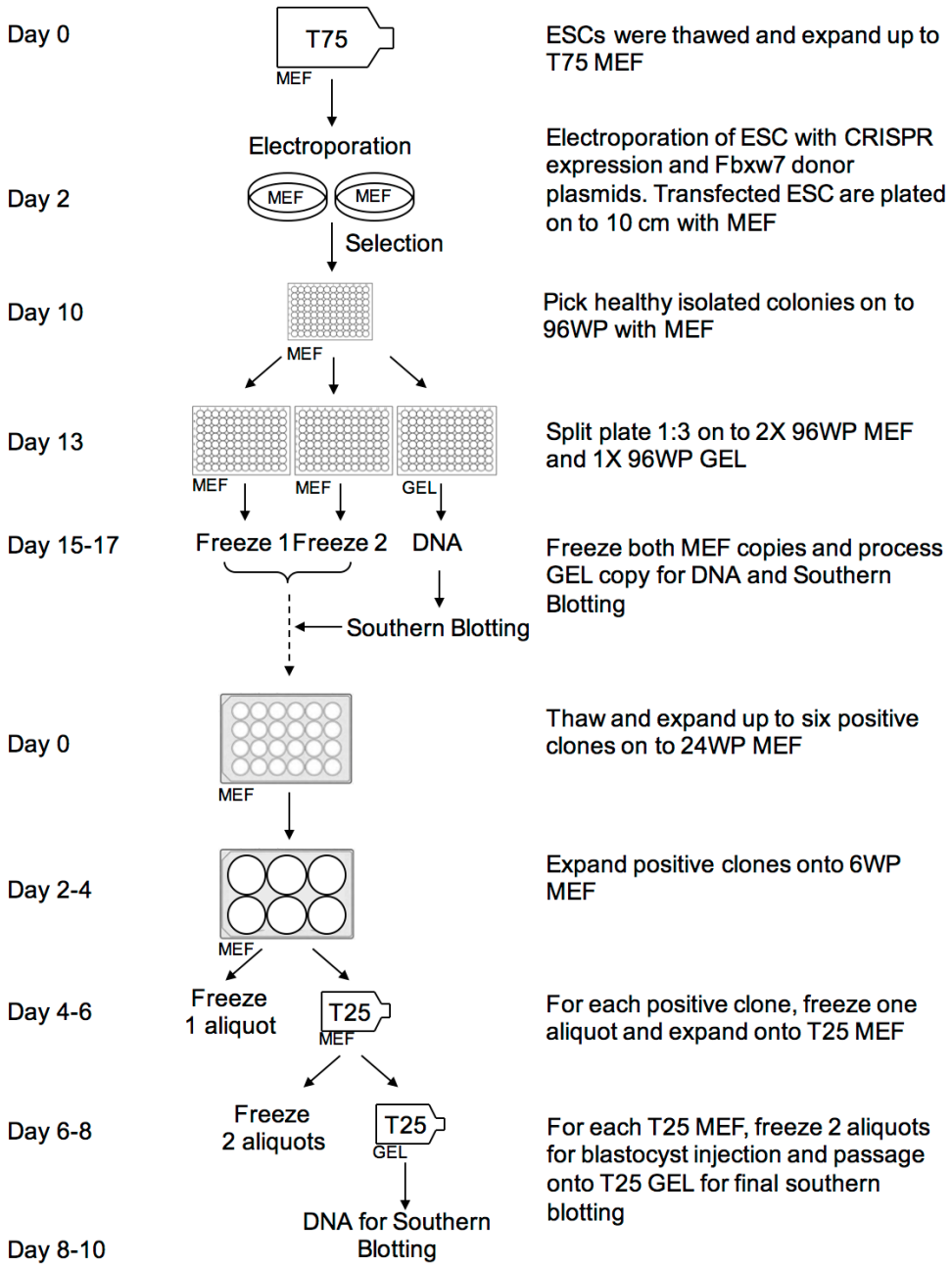

Figure C.2 Embryonic stem culture procedures and timeline.